



# LUND UNIVERSITY

## Optimisation of image quality and radiation dose in computed tomography using iterative image reconstruction

Aurumskjöld, Marie-Louise

2017

*Document Version:*

Publisher's PDF, also known as Version of record

[Link to publication](#)

*Citation for published version (APA):*

Aurumskjöld, M.-L. (2017). *Optimisation of image quality and radiation dose in computed tomography using iterative image reconstruction*. [Doctoral Thesis (compilation), Medical Radiation Physics, Malmö]. Lund University: Faculty of Medicine.

*Total number of authors:*

1

### General rights

Unless other specific re-use rights are stated the following general rights apply:

Copyright and moral rights for the publications made accessible in the public portal are retained by the authors and/or other copyright owners and it is a condition of accessing publications that users recognise and abide by the legal requirements associated with these rights.

- Users may download and print one copy of any publication from the public portal for the purpose of private study or research.
- You may not further distribute the material or use it for any profit-making activity or commercial gain
- You may freely distribute the URL identifying the publication in the public portal

Read more about Creative commons licenses: <https://creativecommons.org/licenses/>

### Take down policy

If you believe that this document breaches copyright please contact us providing details, and we will remove access to the work immediately and investigate your claim.

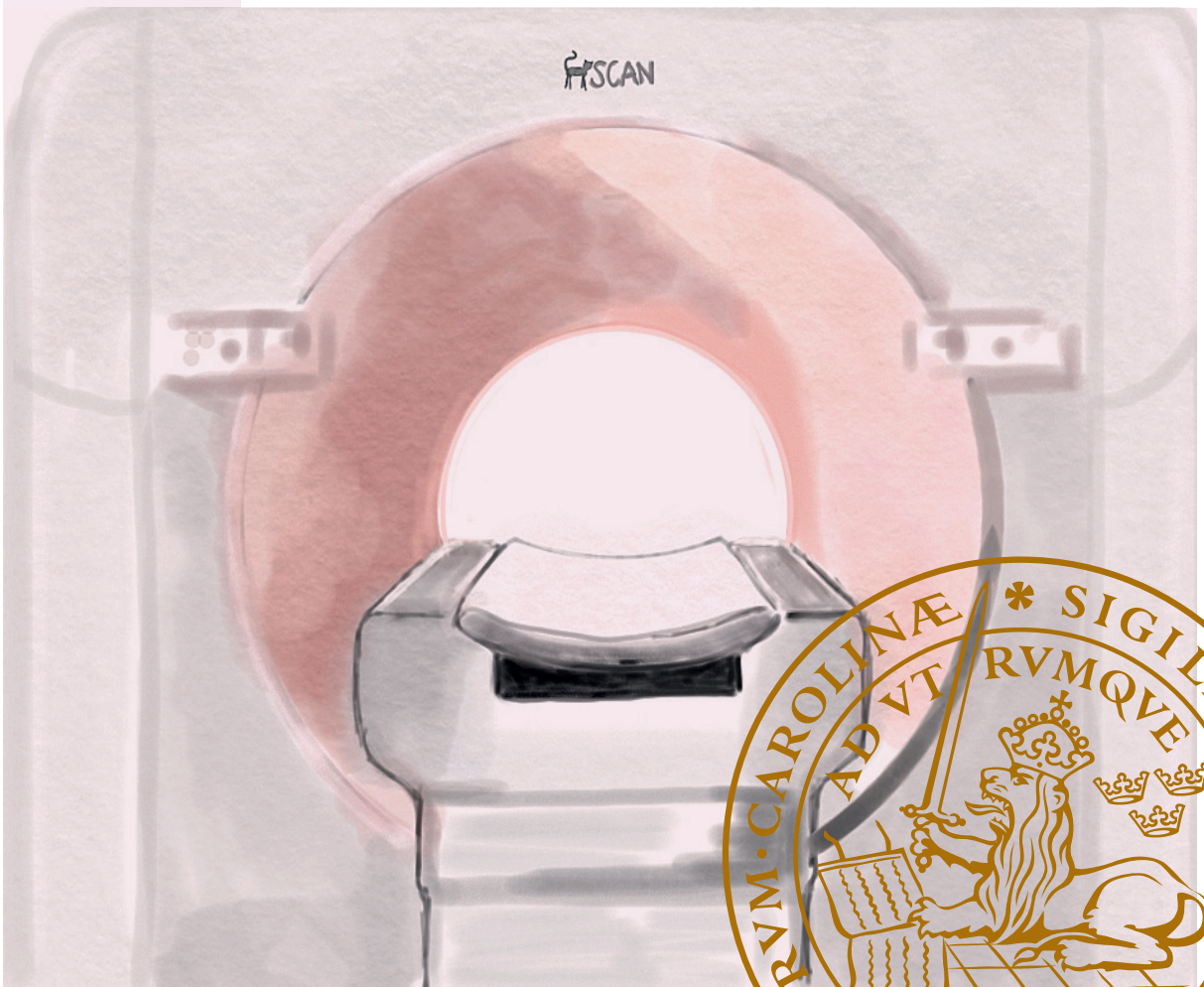
LUND UNIVERSITY

PO Box 117  
221 00 Lund  
+46 46-222 00 00

# Optimisation of image quality and radiation dose in computed tomography using iterative image reconstruction

MARIE-LOUISE AURUMSKJÖLD

MEDICAL RADIATION PHYSICS MALMÖ | LUND UNIVERSITY





# Optimisation of image quality and radiation dose in computed tomography using iterative image reconstruction

Marie-Louise Aurumskjöld



**LUND**  
UNIVERSITY

DOCTORAL DISSERTATION

by due permission of the Faculty of Medicine, Lund University, Sweden.  
To be defended at Jubileumsaulan, MFC, SUS, Malmö. 2017-09-22, 09:00.

*Faculty opponent*

Associate professor Håkan Geijer,  
Örebro University Hospital, Örebro University, Sweden

|   |  |                        |
|---|--|------------------------|
| Organization<br>LUND UNIVERSITY   | Document name<br>DOCTORAL DISSERTATION |                        |
|   | Date of issue                          |                        |
| Author(s) Marie-Louise Aurumskjöld  | Sponsoring organisation                |                        |
| Title and subtitle: Optimisation of image quality and radiation dose in computed tomography using iterative image reconstruction  |  |                        |
| <p>Abstract</p> <p><b>Background:</b> Computed tomography (CT) is one of the most important diagnostic tools for medical imaging. CT is known as a high-dose modality and for producing images that allow for high diagnostic confidence. The challenge is to establish an optimal image quality for the specific diagnostic task with regard to the lowest radiation dose to the patient. Various technological advances have been introduced to reduce radiation dose in CT, such as iterative reconstruction (IR) of the images.</p> <p><b>Aims:</b> The overall aim of this thesis is to investigate and evaluate IR algorithms in terms of image quality and radiation dose, and in clinical practise to evaluate the potential of a new model-based IR (MBIR) method for reconstructing paediatric abdominal CT examinations at a reduced radiation dose.</p> <p><b>Material and methods:</b> The image quality for six IR algorithms in four CT systems of brain CT was evaluated with an image quality phantom using different radiation dose levels and iterative image optimisation levels (Paper I). Philips IR and MBIR were further investigated for abdominal CT (Paper II) with regard to image quality and radiation dose. An image quality phantom and an anthropomorphic torso phantom were used to investigate how image quality depends on IR and MBIR variations with different radiation dose levels and tube voltages. Philips MBIR was investigated with thinner slice thickness and compared with standard slice thickness with IR for abdominal CT (Paper III). This study included investigation of image quality in both the image quality phantom and anthropomorphic phantom and one clinical case. An investigation of Philips MBIR was performed with paediatric abdominal CT involving a 32% lower radiation dose compared to the standard examination (Paper IV). Various approaches for subjective and objective evaluation of image quality were used and assessed.</p> <p><b>Results:</b> In this thesis, the effects on image quality and radiation dose from the use of advanced reconstruction methods for CT was investigated in both phantoms and patients. The IR algorithms have different strengths and weaknesses, and in conclusion all IR algorithms improved the main part, or all of the image quality parameters compared to filtered back projection. For all IR algorithms, subjective image quality was improved. The objective image quality parameters; noise, signal-to-noise ratio, and contrast-to-noise ratio were all improved although to a variable degree. Spatial resolution was improved only for MBIR algorithms and GE IR (adaptive statistical iterative reconstruction). The IR algorithms improved image quality regardless of radiation dose. The MBIR algorithms improved image quality progressively with decreasing radiation dose but affected the image appearance, which can be attributed to a change in the noise power spectrum. For Philips MBIR (IMR), it is possible to use thinner slice thickness with maintained or even improved image quality. Furthermore, with Philips MBIR (IMR), it is possible to reduce the radiation dose and improve low-contrast resolution for low-contrast scanning in both brain and abdomen. A dose reduction of 32% with IMR in paediatric abdominal CT was possible without degradation of image quality. There is great potential to lower radiation dose by using IR and MBIR.</p> <p><b>Conclusion:</b> The radiation dose can be reduced with new iterative reconstruction methods while maintaining or in some cases improving image quality compared to older reconstruction methods.</p> |  |                        |
| Key words: Computed tomography, iterative reconstruction, image quality, radiation dose, CT brain, CT abdomen, paediatric, slice thickness  |  |                        |
| Classification system and/or index terms (if any)   |  |                        |
| Supplementary bibliographical information   |  | Language: English      |
| ISSN and key title 1652-8220  |  | ISBN 978-91-7619-499-7 |
| Recipient's notes   | Number of pages 61                     | Price                  |
|   | Security classification                |                        |

I, the undersigned, being the copyright owner of the abstract of the above-mentioned dissertation, hereby grant to all reference sources permission to publish and disseminate the abstract of the above-mentioned dissertation.

Signature



Date 2017-08-17

# Optimisation of image quality and radiation dose in computed tomography using iterative image reconstruction

Marie-Louise Aurumskjöld



**LUND**  
UNIVERSITY

Cover illustration front: by Marie-Louise Aurumskjöld

Cover illustration back: by Matz Nilsson, photograph of the author 2017.

Copyright Marie-Louise Aurumskjöld (pages 1-61)

Faculty of Medicine  
Department of Translation Medicine  
Medical Radiation Physics Malmö  
Skåne University Hospital  
SE-205 02 Malmö

ISBN 978-91-7619-499-7

ISSN 1652-8220

Lund University, Faculty of Medicine Doctoral Dissertation Series 2017:116

Printed in Sweden by Media-Tryck, Lund University  
Lund 2017



*Dedicated to my beloved family*

# Contents

|   |    |
|---|----|
| Summary .....   | 8  |
| Sammanfattning (in Swedish) .....                               | 10 |
| Abbreviations .....   | 12 |
| Original papers .....   | 13 |
| Other related presentations and publications by the author..... | 14 |
| Introduction .....  | 15 |
| Background .....  | 17 |
| The basic principles of CT .....                                | 17 |
| Image reconstruction .....                                      | 18 |
| The principles of FBP.....                                      | 18 |
| The principles of IR.....                                       | 19 |
| Image quality.....  | 24 |
| Low-contrast resolution.....                                    | 25 |
| High-contrast resolution .....                                  | 26 |
| Image artifacts .....   | 26 |
| Subjective evaluation of image quality .....                    | 27 |
| Radiation dose and risks in CT imaging .....                    | 28 |
| Radiation dose .....  | 28 |
| Radiation risk .....  | 29 |
| Aims .....  | 31 |
| Paper I .....   | 31 |
| Paper II.....   | 31 |
| Paper III.....  | 31 |
| Paper IV .....  | 31 |

|  |    |
|--|----|
| Material and Methods.....                  | 33 |
| Overview.....                              | 33 |
| Scanning technique.....                    | 35 |
| Image reconstruction.....                  | 36 |
| Image quality assessment.....              | 37 |
| Results and discussion.....                | 41 |
| Image quality.....                         | 41 |
| Noise and spatial resolution.....          | 41 |
| Low-contrast resolution.....               | 43 |
| Slice thickness.....                       | 43 |
| Noise power spectrum.....                  | 44 |
| CT numbers.....                            | 46 |
| Artifacts.....                             | 47 |
| Radiation dose.....                        | 47 |
| Clinical implementation.....               | 48 |
| Summary of results.....                    | 49 |
| Conclusion.....                            | 51 |
| Future aspects of this research field..... | 51 |
| Acknowledgements.....                      | 53 |
| References.....                            | 55 |

# Summary

Today, computed tomography (CT) is one of the most important diagnostic tools in modern health care. The examination with a CT is fast, available 24 hours a day, and can be used for almost all patients. CT is known as a high-dose modality but also produces images with high diagnostic value. The role of accurate investigation and diagnosis in the management of all diseases is unquestionable. Every examination with ionising radiation should be performed according to the ALARA principle (As Low As Reasonably Achievable), meaning that the examination should be performed with a balance obtaining the necessary diagnostic information while keeping the radiation dose to the patient as low as possible.

Dose reduction in CT often results in degradation of the image quality, i.e., higher noise and decreased low contrast resolution. Various technological advances have been introduced to reduce radiation dose in CT, mainly hardware improvement such as better detector material, anti-scatter grid, beam shaping filters, dose modulation and also advanced software solutions such as post-processing image filters and iterative reconstruction (IR) methods. Filtered back projection (FBP) has been the most common reconstruction method but is increasingly being replaced by different types of IR methods.

The overall objective of this thesis is to evaluate and optimise IR methods in CT regarding image quality and radiation dose to the patient. The areas of major challenge are those that require high low-contrast resolution, such as imaging of brain, liver and paediatric investigations. Hence, the focus has been on these areas. In the case of children, it is especially important to keep the radiation dose as low as possible without jeopardising the diagnostic accuracy, bearing in mind the increased risk of radiation-induced cancer resulting from exposure to ionising radiation at young ages. The thesis includes a combination of studies on phantoms and patients for evaluation of the impact of IR algorithms with regard to image quality and radiation dose.

Paper I: Six different IR algorithms were evaluated in brain CT using different combinations of radiation dose levels and IR/MBIR levels (also called reconstruction strengths). An image quality phantom, supplied with a bone-mimicking ring to simulate the beam-hardening effects created by the skull, was used. Image quality was evaluated in terms of CT number, uniformity, noise, noise power spectra, low-contrast resolution, and spatial resolution.

Paper II: Objective and subjective evaluations of image quality was evaluated for an image quality phantom with and without an oval-shaped body annulus. The phantom was scanned with different radiation dose levels and images were reconstructed with different IR/MBIR levels. The annulus was used to better

simulate the size and shape of humans. In addition, an anthropomorphic torso phantom was used for assessment of image noise and contrast-to-noise ratio for the liver/vessel.

Paper III: The impact of the slice thickness of the CT images reconstructed with IR and MBIR was investigated for standard protocol for CT abdomen. An image quality phantom, an anthropomorphic phantom, and one clinical case were used to assess image quality for different IR/MBIR levels and slice thicknesses.

Paper IV: Investigation of whether MBIR could maintain or improve the image quality of paediatric abdominal CT examinations compared to the current IR method, when the radiation dose was reduced. Twenty patients were examined with standard dose settings, and twenty patients were examined with 68% of the radiation dose. Image quality was evaluated subjectively by three observers, and image noise in the liver was measured.

IR algorithms have different strengths and weaknesses, but the important conclusion from all studies in this thesis is that all vendors' iterative reconstruction algorithms improve image quality compared to FBP for the same radiation dose. Subjective image quality was improved. Noise, signal-to-noise, and contrast-to noise were all improved although to different degrees. For Philips IMR (MBIR), it is possible to use thinner slice thickness and maintain or even improve image quality. With IMR, it is also possible to reduce the radiation dose and improve low-contrast resolution for low-contrast scanning such as brain and abdominal CT scans.

## Sammanfattning (in Swedish)

Datortomografi (DT) är idag ett av de viktigaste verktygen inom sjukvården för att ställa korrekta diagnoser. En undersökning med DT går snabbt att göra, utrustningen är tillgänglig dygnet runt och kan användas på nästan alla patienter. DT ger ofta höga stråldoser men fördelen är att den producerar bilder med hög diagnostisk kvalitet.

Undersökningar med joniserande strålning skall genomföras enligt ALARA-principen (As Low As Reasonably Achievable), vilket innebär att undersökningen ska genomföras på ett sätt så att man får tillräckligt god diagnostisk information samtidigt som stråldosen till patienten är så låg som rimligen är möjligt. Detta kräver en balans mellan stråldos och bildkvalitet. En sänkning av stråldosen av en DT-undersökning medför oftast en sämre bildkvalitet, dvs. högre brus och sämre lågkonstrast-upplösning. Olika tekniska förbättringar har under senare år gjorts och detta medför att man kan reducera stråldosen inom DT. Exempel på sådana är bättre detektormaterial, anti-scatter grid (raster), olika typer av filtrering av röntgenstrålen, exponeringsautomatik och även avancerade mjukvaror som filter vid bildbehandling samt iterativ rekonstruktion (IR). Filtrerad bakåtprojektion (FBP) har varit den vanligaste metoden för rekonstruktion av DT-bilder, men har mer och mer ersatts av IR-metoder.

Det övergripande målet med avhandlingen är att utvärdera IR-metoder för DT och optimera dessa med avseende på bildkvalitet och patientstråldos. Den största utmaningen att sänka stråldosen är för de undersökningar som kräver god lågkonstrast som till exempel hjärna, lever och vid pediatrika undersökningar. Fokus på arbetet i avhandlingen har därför lagts på dessa områden. När det gäller barn är det extra viktigt att hålla stråldosen så låg som möjligt utan att äventyra den diagnostiska informationen, detta med tanke på att barn har en ökad risk för strålningsinducerad cancer. Avhandlingen innehåller studier på både fantom och patienter och där effekten av olika IR-metoder utvärderas med avseende på bildkvalitet och stråldos.

I den första studien utvärderades sex olika IR-metoder för DT-hjärna för olika stråldosnivåer och nivåer på IR. Ett bildkvalitetsfantom användes i kombination med en bensimulerande ring för att efterlikna de effekter man får av skallben (beam-hardening). De bildkvalitetsparametrar som utvärderades i studien var DT-värde, homogenitet, brus, noise-power-spektrum, lågkonstrast och spatiell upplösning.

Den andra studien utvärderade en IR och en modellbaserad IR (MBIR) i kombination med olika stråldosnivåer och rekonstruktionsnivåer för DT-buk. I studien användes ett bildkvalitetsfantom med och utan en ovalformad kroppsring, detta för att bättre simulera en människas storlek och form. Både objektiv och

subjektiv utvärdering av bildkvaliteten gjordes. Dessutom användes ett antropomorfiskt torsofantom för bedömning av brus och kontrast-till-brusförhållandet för lever/kärl i DT-bilderna.

I den tredje studien utvärderades betydelsen av snittjocklek på de rekonstruerade DT-bilderna av buk då IR och MBIR används. För bedömningen användes bildkvalitetsfantom, ett antropomorfiskt torsofantom samt en patient. Studien gjordes på en standardundersökning av DT-buk och bildkvaliteten utvärderades för olika snittjocklekar och olika IR/MBIR-rekonstruktionsnivåer.

I den sista studien i avhandlingen undersöktes om det är möjligt att sänka stråldosen och använda MBIR med bibehållen eller förbättrad bildkvalitet vid DT-bukundersökning på barn, jämfört med nuvarande IR-metod. Tjugo patienter undersöktes med standardundersökningen och bilderna rekonstruerades med standard IR-metod. Tjugo patienter undersöktes med 68 % av stråldosen och bilderna rekonstruerades både med standard IR och med MBIR. Bildkvaliteten utvärderades subjektivt av tre observatörer och dessutom mättes brus i levern.

IR-metoderna har olika styrkor och svagheter, och den viktigaste slutsatsen av alla studierna är att alla leverantörers IR-metoder förbättrar bildkvaliteten jämfört med FBP för samma stråldos. Subjektiv bildkvalitet förbättrades. Brus, signal-till-brus och kontrast-till-brus förbättrades för alla iterativa metoder, men i olika grad. För MBIR (Philips IMR) är det möjligt att använda tunnare snittjocklek och bibehålla eller till och med förbättra bildkvaliteten. Med IMR är det också möjligt att minska stråldosen och förbättra lågkonstrastupplösningen för undersökningar såsom DT-hjärna och DT-buk.

# Abbreviations

|        |  |
|--------|--|
| AAPM   | American Association of Physicists in Medicine       |
| AIDR   | Adaptive Iterative Dose Reduction (Toshiba)          |
| ALARA  | As Low As Reasonably Achievable                      |
| ART    | Algebraic Reconstruction Technique                   |
| ASIR   | Adaptive Statistical Iterative Reconstruction (GE)   |
| AUC    | Area Under the Curve                                 |
| CNR    | Contrast-to-Noise Ratio                              |
| CI     | Confidence Interval                                  |
| CT     | Computed Tomography                                  |
| CTDI   | Computed Tomography Dose Index                       |
| DLP    | Dose Length Product                                  |
| FBP    | Filtered Back Projection                             |
| HU     | Hounsfield Unit                                      |
| ICC    | Intraclass Correlation Coefficient                   |
| ICRP   | International Commission on Radiological Protection  |
| IEC    | International Electrotechnical Commission            |
| IMR    | Iterative Model Reconstruction (Philips)             |
| IR     | Iterative Reconstruction                             |
| IRIS   | Iterative Reconstruction in Image Space (Siemens)    |
| MBIR   | Model-Based Iterative Reconstruction                 |
| MTF    | Modulation Transfer Function                         |
| NPS    | Noise Power Spectrum                                 |
| ROC    | Receiver Operating Characteristics                   |
| ROI    | Region Of Interest                                   |
| SAFIRE | Sinogram Affirmed Iterative REconstruction (Siemens) |
| SD     | Standard Deviation                                   |
| SNR    | Signal-to-Noise Ratio                                |
| VGC    | Visual Grading Characteristics                       |

## Original papers

This thesis is based on the following four papers, which are referred to in the text by their Roman numerals. The papers are appended at the end of the thesis.

- Ia. *Six iterative reconstruction algorithms in brain CT: a phantom study on image quality at different radiation dose levels*  
Löwe A, Olsson M-L<sup>1</sup>, Siemund R, Stålhammar F, Björkman-Burtscher I and Söderberg M  
Br J Radiol, 2013; 86: 20130388
- Ib. *Clinically essential requirement for brain CT with iterative reconstruction: author reply*  
Löwe A, Olsson M-L<sup>1</sup>, Siemund R, Stålhammar F, Björkman-Burtscher I and Söderberg M  
Br J Radiol, 2014; 87(1044): 20140533
- II. *Improvements to image quality using hybrid and model-based iterative reconstructions: a phantom study*  
Aurumskjöld M-L, Ydström K, Tingberg A and Söderberg M  
Acta Radiol, 2017; 58(1): 53-61
- III. *Model-based iterative reconstruction enables the evaluation of thin-slice computed tomography images without degrading image quality or increasing radiation dose*  
Aurumskjöld M-L, Ydström K, Tingberg A and Söderberg M  
Rad Prot Dosim, 2015; 169(1-4): 100-106
- IV. *Evaluation of an iterative model-based reconstruction of pediatric abdominal CT, with regard to image quality and radiation dose*  
Aurumskjöld M-L, Söderberg M, Stålhammar F, Vult von Steyern K, Tingberg A and Ydström K  
Acta Radiol, 2017 August, DOI: 10.1177/0284185117728415  
(Epub ahead of print)

Published papers have been reproduced with kind permission of the following publishers:

The British Institute of Radiology (Paper Ia, Paper Ib)

The Royal Society of Medicine Press Ltd (Paper II and Paper IV)

Oxford University Press (Paper III)

<sup>1</sup>Marie-Louise Olsson changed her name to Marie-Louise Aurumskjöld in June 2014.

## Other related presentations and publications by the author

*An investigation of iterative reconstruction method iDose<sup>4</sup> on a Philips Brilliance 64 using a Catphan 600 phantom*

Olsson M-L<sup>1</sup> and Norrgren K<sup>2</sup>  
Proc SPIE 8313; Medical Imaging, 2012

*An investigation of iterative reconstruction method iDose<sup>4</sup> with Catphan 600 on Philips CT Brilliance 64*

Olsson M-L<sup>1</sup>, Norrgren K<sup>2</sup> and Söderberg M  
Proc European Congress of Radiology, 2014

*Model-based iterative reconstruction IMR gives possibility to evaluate thinner slice thicknesses than conventional iterative reconstruction iDose<sup>4</sup>: a phantom study*

Aurumskjöld M-L, Ydström K, Tingberg A and Söderberg M  
Proc SPIE 8313; Medical Imaging, 2015

*Improvement of CT image quality with iterative reconstruction iDose<sup>4</sup>*

Aurumskjöld M-L, Ydström K and Söderberg M  
Proc European Congress of Radiology, 2016

<sup>1</sup>Marie-Louise Olsson changed her name to Marie-Louise Aurumskjöld in June 2014.

<sup>2</sup> Kristina Norrgren changed her name to Kristina Ydström in December 2014.

# Introduction

The role of accurate investigation and diagnosis in the management of all diseases is unquestionable. Medical imaging provides not only a basis for diagnosis but also for planning and monitoring the treatment of diseases. Imaging with ionising radiation is a permanent feature of medical diagnostics. Around 1957, Allan M. Cormack developed the theoretical basis for computed tomography (CT). In 1966–1972, Godfrey N. Hounsfield developed CT (Hounsfield, 1973). Cormack and Hounsfield were awarded the Nobel Prize in physiology or medicine 1979 for the development of CT. The word “tomo” is from a Greek word and means “slice, section”. In older terminology, the equipment was also called CAT scan, short for computer-aided tomography scan or computerised axial tomography scan. Today, CT is one of the most important diagnostic tools in the hospital. CT is available 24 hours a day, is fast, and can be used for almost all patients. A CT examination is typically a high-dose examination, but the advantage is images with high diagnostic value. CT image reconstruction is much more complicated than conventional planar X-ray imaging. In CT, registered transmitted X-rays are reconstructed with extensive image-reconstruction algorithms to form the images.

A continuous increase in CT examinations performed per year has raised concerns over the risk associated with the increased collective effective dose (Almén et al., 2008; International Commission on Radiological Protection [ICRP] 2000, ICRP 2007a). CT has become an integral part of paediatric imaging, and the risk of radiation-induced cancer is higher for children than adults (Shah et al., 2008; Miglioretti et al., 2011; Miglioretti et al., 2013). Children are not small adults and differ considerably from adults in terms of body composition, anatomy, and proportions. Various organ systems are age-dependent in children (ICRP, 1991); limb bones contain hematopoietic marrow, bones are more cartilaginous than in adults, and there is less overlying muscle and structural fat. Thus, the radiographic density decreases and density differences are less pronounced. Considering the difference in body composition and anatomy, children have specific needs in CT image quality and require dedicated scanning protocols, separated from optimisation of examination protocols of adults.

The challenge is to establish an optimal image quality for the specific diagnostic task at the lowest radiation dose to the patient. Maintaining image quality while reducing radiation dose is a major technical challenge. Dose reduction in CT often

results in degradation of image quality. Various technological advances have been introduced to reduce radiation dose in CT, mainly hardware improvements such as detector material, anti-scatter grid, different types of filters, and dose modulation, but also advanced software solutions such as post-processing image filters and iterative reconstruction (IR) (Kalender et al., 2008).

Filtered back projection (FBP) has been the industry standard for CT image reconstruction for decades. FBP is a fast and robust method but is suboptimal for poorly sampled data or cases with high noise such as low-dose scans or scans on obese patients (Pan et al., 2009; Fleischmann et al., 2011; Nelson et al., 2011). An evolution to more advanced IR algorithms that may allow reduction of the radiation dose and improvement of image quality was the next step in CT technology (Funama et al., 2011; Gervaise et al., 2012; Prakash et al., 2010; Winklehner et al., 2011). These advanced algorithms have been used in single-photon emission computed tomography and positron-emission tomography for many years. In CT imaging, reconstruction time is crucial, and previously IR was clinically unacceptable. With new computational hardware, it is now possible to use IR in the clinical routine. New algorithms are constantly being developed and need to be evaluated for clinical use.

The overall objective of this thesis was to evaluate and optimise IR methods in CT regarding image quality and radiation dose to the patient. Areas of major challenge are those that require high low-contrast resolution, such as imaging of brain and liver and paediatric investigations. Hence, the focus has been on these areas. In the case of paediatric patients, it is especially important to keep the radiation dose as low as possible while not jeopardising diagnostic certainty.

# Background

## The basic principles of CT

During image acquisition, the X-ray tube and the detector continuously rotate around the patient. There are two types of scanning, sequential (axial) and spiral. Sequential involves one complete rotation followed by a table movement, the so-called “step and shoot”. In spiral mode, the table moves continuously through the gantry during acquisition. The pitch value describes the table motion and is defined as the ratio between the table transportation per rotation and the collimated beam width. An increased pitch allows a faster scan and reduces the radiation dose if all other parameters are kept constant. The image quality will be affected in terms of increased noise and decreased low contrast resolution as well as reduced spatial resolution along the body (z-axis) caused by inconsistent projection data.

After the introduction of multi-detector CT in 1996, the coverage of the patient per rotation has rapidly increased, thus reducing examination time (Kopp et al., 2000). The most common detector configuration today is from 64 to 320 detector rows. Every CT slice is subdivided into a matrix (e.g., 512×512 or 1024×1024). Each element (voxel) has been traversed by numerous X-ray photons, and the transmitted radiation is measured by the detector.

The attenuation of a monochromatic narrow X-ray beam passing through a homogeneous material is described by the following equation:

$$I = I_0 e^{-\mu x} \quad (1)$$

where  $I$  is the number of photons behind the object,  $I_0$  is the number of photons at the same point in the absence of the object,  $x$  is the object thickness, and  $\mu$  is the linear attenuation coefficient of the material for the photon energy used. The linear attenuation coefficient  $\mu$  is strongly dependent on the photon energy and therefore only of limited use for characterising the radiation attenuation capacity of an object in CT. The attenuation value in CT (Hounsfield unit; HU) is the scaled difference of the linear attenuation coefficient of the investigated object from the linear attenuation coefficient of water. Water is used as the reference material:

$$HU = k \frac{\mu_{object} - \mu_{water}}{\mu_{water} - \mu_{air}} \quad (2)$$

where  $k$  is 1000 and  $\mu_{\text{water}}$  and  $\mu_{\text{air}}$  are the linear attenuation coefficients of water and air.

Specific attenuation values are assigned to each individual voxel. The reconstructed image consists of a matrix of picture elements, or pixels. Each pixel is assigned a numerical value (HU), which is the average of all attenuation values within the voxel (equation 2). This scale assigns water an attenuation value of 0 HU and air -1000 HU. Each number represents a shade of grey with -1000 HU (black) to +1000 HU (white). By using so-called windowing technique (window widths and levels), certain types of tissues can be viewed in more detail.

## Image reconstruction

Different approaches are available to calculate the slice image from a CT. Calculating each pixel value in the image requires independent equations, and one equation can be written for each measurement. A particular sample in a particular profile is the sum of a particular group of pixels in the image. When overdetermined in this manner, the final image has reduced noise and artefacts. When reconstructing an image of  $512 \times 512$  matrix size, however, the CT system might take 700 views with 600 samples in each view. The great problem with this method of CT reconstruction is to solve several hundred thousand equations, which previously was next to impossible (Smith, 1997).

The most common CT reconstruction methods can be classified into two distinct groups: filtered back projection methods and iterative reconstruction. The method of FBP or convolution and back projection was the most common reconstruction method until recently. All major CT vendors have one or two types of IR methods available today. IR is not a new invention because this method was used to reconstruct the first CT images in the early 1970s (Hounsfield, 1973).

### **The principles of FBP**

In FBP, also referred to as convolution back projection, the projections are smeared back across the image at the acquisition angle and summed to obtain an approximation of the original image (Kak et al., 1988). Star-shaped artifacts will appear in the resulting image by this process. Use of a high-pass filter allows reduction of these artifacts. The method relies on the relationship dedicated by the Fourier Slice Theorem (Kak et al., 1988). This method is computationally fast and has been the most commonly used method in tomographic reconstruction.

FBP corrects for the blurring that is present in the simple back projection. To counteract the blurring, each view is filtered before back projection is applied. The filtered views are then back projected to provide the reconstructed CT image. The reconstructed CT image is identical to the “correct” image if there is an infinite number of views and an infinite number of points per view, and it is assumed that the focal spot is infinitely small and the dimension of the detector elements is ignored.

## **The principles of IR**

The reconstruction method used in the first commercial medical CT scanner was the algebraic reconstruction technique (ART) (Gordon et al., 1970). The size of these systems of equations is usually large, which resulted in unsustainable calculation times in image CT reconstructions. There are several variations of IR methods, and each vendor has their own solution. The difference lies in how the successive calculations and corrections are made, ray-by-ray, pixel-by-pixel, or by simultaneously correcting the entire data set.

ART starts with all pixels in the image array set to arbitrary values, which the iterative procedure then uses to gradually change the image array to correspond to the profiles. The measured sample is compared with the sum of the image pixels along the X-ray path. If the sum is lower than the measured sample, all pixel values in this path are increased. If the sum is higher, the correction will be made by decreasing the pixel values. After the first iteration cycle, there will still be errors between the sum of image pixel values and the measured values. With this method, the errors become smaller with repeated iterations.

### *Statistical or hybrid IR*

IR algorithms iterated in both raw data domain and image data domain are designated as statistical or hybrid IR. The statistical/hybrid IR models the electronic and photon noise in the measured data. No new information will appear in the data set after reconstruction, so this method will only suppress the noise. The potential benefit is that it is possible to improve the image quality and/or lower the radiation dose. IR will allow imaging at lower radiation doses with similar noise levels and image quality compared to routine-dose FBP. Dose reduction may be achieved without compromising the image quality. An illustration of how statistical/hybrid IR can work is shown in Figure 1.

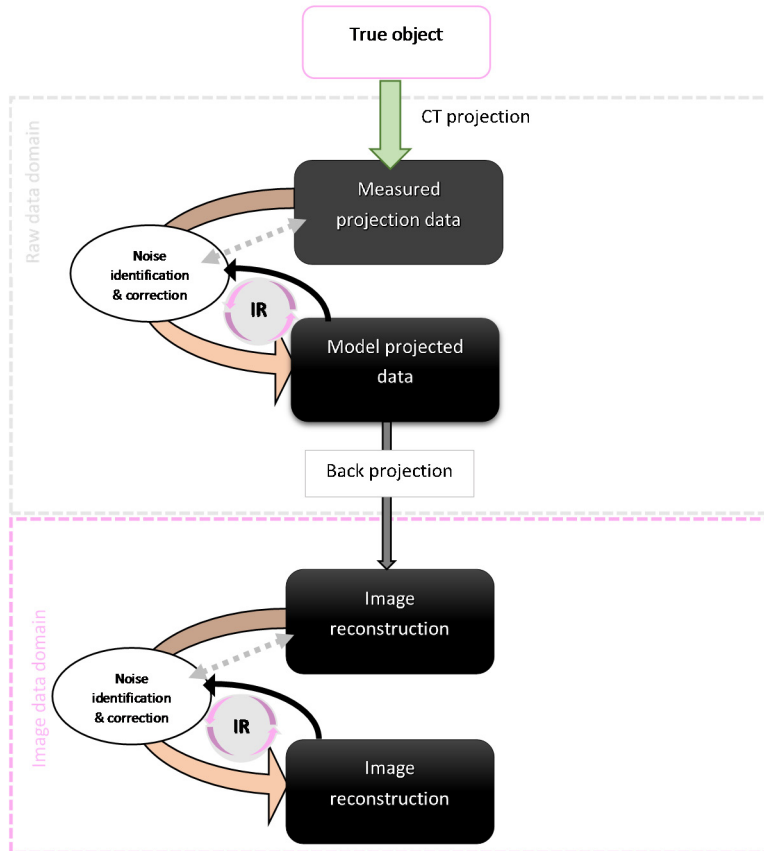


**Figure 1.** Exampel overview of hybrid/statistical iterative reconstruction (IR) technique. A noise correction is applied both in the raw data and the image domain. The IR algorithm first identifies and corrects the noisiest raw data, preserving edges using maximum likelihood, and denoising algorithm based on Poission statistics. The next step is that the corrected raw data are reconstructed with back projection into the image domain. Then uncorrelated noise is iteratively decreased in the reconstructed image (vendors use similar approaches).

### *Model-based IR*

In model-based IR (MBIR), or full IR, the imaging system and the true object as well as the noise in the projection data are modelled (Thibault, 2010; Metha, 2013). The first reconstruction step is a normal FBP, performed to reconstruct a CT image model of the object. The CT image is propagated into the raw data domain by a forward reconstruction step, simulating CT acquisition and using a priori knowledge of the characteristics of the CT system (e.g., electronic noise, detector characteristics and system geometry). After comparison to the measured projection data, corrections are made based on the object and noise models, and the object model is propagated back to the image data domain by backward reconstruction. Forward

and backward reconstruction steps are repeated a fixed number of times or until corrections become very small. In an ideal situation, the noise can simply be removed from the modelled projection data in a final reconstruction step, resulting in an artifact- and noise-free image. With a proper simulation of the CT system, the MBIR allows reduction of image quality artifacts resulting from common irregularities like beam hardening, photon starvation, and nonlinearity of individual detector elements (Willemink et al., 2013). An illustration of how MBIR can work is shown in Figure 2.

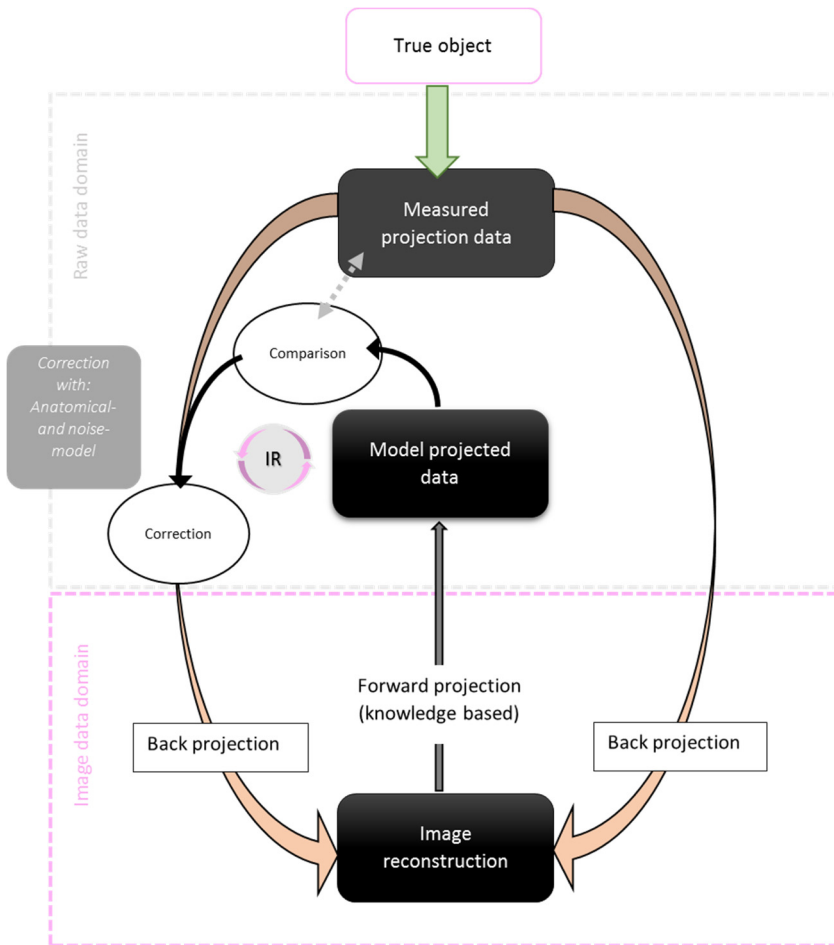


**Figure 2.** Overview of a model-based iterative reconstruction (MBIR) technique. MBIR consists of both backward and forward reconstruction steps with a knowledge-based correction and correction for an anatomical- and noise-model (commercially available at Philips MBIR; IMR).

### *Vendor-specific IR approaches*

Since the reintroduction of the first commercially available IR algorithms in 2008 (Hsieh, 2008), the development of the algorithms has progressed rapidly. All leading manufacturers of CT systems offer more than one type of IR solution. Detailed information of the IR algorithms is not publicly available because it is proprietary information, but algorithms can be divided into the two groups described above, IR and MBIR. The IR are often available in different strength levels (level of noise reduction); for example, GE IR (ASIR) offers the possibility to blend IR images with FBP images from 0–100% (ASIR 0% equals to FBP 100% and ASIR 100% equals FBP 0%), and Philips IR (iDose<sup>4</sup>) has seven levels, with level one corresponding to 11% noise reduction and level seven to 55% noise reduction. Siemens IR (SAFIRE) has five strength levels, where 1 corresponds to the lowest and 5 to the highest strength, and Toshiba IR (AIDR 3D) is available in four levels (mild, standard, strong and enhanced). For MBIR, GE (Veo) and Toshiba (FIRST), have no adjustable strengths available, but Philips (IMR) has three levels available (1 corresponds to low strength and 3 to highest) and Siemens (ADMIRE) has five levels available (1 corresponds to low and 5 to the highest strength).

An overview of the commercially available IR/MBIR reconstruction techniques is shown in Table 1. Reported dose reductions according to the vendors are based on vendors' white papers and information brochures (Hsieh, 2008; Thibault, 2010; Angel, 2012; Grant, 2012; Metha; 2013), shown in Table 1.

**Table 1.**

Commercially available IR algorithms. Less-advanced IR in the image domain alone (image-based IR) is available only from Siemens (IRIS). The statistical/hybrid iterative reconstruction algorithms are abbreviated as IR and the model-based iterative reconstruction as MBIR.

| Vendor  | Acronym            | Full name   | Reconstruction | Year | <sup>1</sup> Theoretical maximal dose reduction according to vendor | <sup>1</sup> Reported dose reduction                          |
|---------|--------------------|---|----------------|------|---|---|
| GE      | ASIR               | Adaptive Statistical Iterative reconstruction                   | IR             | 2008 | 40%   | 23–76% (Sagara et al., 2010; Yanagawa, et al., 2012)          |
|         | ASIR-V             | Adaptive Statistical Iterative reconstruction-V                 | IR             | 2014 | 82%   | 13–35% compared to ASIR (Kwon et al., 2015; Kim et al., 2017) |
|         | Veo                | Product name  | MBIR           | 2010 | 75%   | 50% (Samei et al., 2015)                                      |
| Philips | iDose <sup>4</sup> | Product name  | IR             | 2009 | 80%   | 50–76% (Funama et al., 2011; Habets et al., 2012)             |
|         | IMR                | Iterative Model Reconstruction                                  | MBIR           | 2013 | 80%   | 75% (Sauter et al., 2016)                                     |
| Siemens | IRIS               | Image Reconstruction in Image Space                             | Image-based IR | 2009 | 60%   | 20–60% (Moscariello et al., 2011; Winklehner et al., 2011)    |
|         | SAFIRE             | Sinogram Affirmed Iterative Reconstruction                      | IR             | 2010 | 60%   | 50% (Moscariello et al., 2011; Winklehner et al., 2011)       |
|         | ADMIRE             | Advanced Modeled Iterative Reconstruction                       | MBIR           | 2013 | 60% compared to SAFIRE  | 75% (Martini et al., 2017)                                    |
| Toshiba | AIDR 3D            | Adaptive Iterative Dose Reduction 3D                            | IR             | 2010 | 75%   | 52% (Gervaise et al., 2012)                                   |
|         | FIRST              | Forward projected model-based Iterative Reconstruction SoluTion | MBIR           | 2015 | 82%   | 28% compared to AIDR 3D (Maeda et al., 2017)                  |

<sup>1</sup> The reported dose reduction depends on the type of CT examination, anatomic region, and method used for calculating the dose reduction.

There are two approaches to optimisation of acquisition data either in the projection domain or in the image domain. Optimisation in the projection domain offers the ability to prevent noise and artifacts.

Image-based IR is a denoising algorithm working in the image domain. The technique was developed to produce lower image noise. Artifacts associated with

significantly lower doses cannot be reduced. This solution is cost effective, with no extra computational requirements, and reconstruction time is roughly the same as for FBP. An example of image-based IR is IRIS from Siemens.

Statistical/hybrid IR, called IR in Table 1, is based on denoising the raw data and image data. These techniques are to a greater extent replacing FBP as the standard method reconstruction in CT. Significant noise reduction and artifact prevention mean that these techniques offer the possibility of reducing the radiation dose while maintaining image quality (Figure 1). Examples of statistical and hybrid IR are ASIR, ASIR-V, iDose<sup>4</sup>, SAFIRE, and AIDR 3D.

MBIR and knowledge-based IR incorporate forward-models of the system geometry, noise, and anatomical model (Figure 2). These processes increase the reconstruction time, but with newer hardware, the reconstruction time can be short enough to be clinically acceptable. Examples of commercially available MBIR are Veo, IMR, ADMIRE, and FIRST.

Table 1 shows the IR/MBIR algorithms that are commercially available today, the theoretical maximum dose reduction according to the vendor, and the reported dose reduction found in the literature. Many published studies describe investigations of the possibility of dose reduction and how the image quality is affected by various IR techniques with patients or phantoms. Dose reduction strongly depends on the applied anatomic region and calculation method. Some studies calculate dose reduction based on reduced image noise (Gervaise et al., 2012). Studies are frequently performed of abdominal CT (Hara et al., 2009; Singh et al., 2010; Kalra et al., 2012; Yasaka et al., 2013; Vardhanabhuti et al., 2014; Aurumskjöld et al., 2017), chest CT (Pontana et al., 2011; Pontana et al., 2011; Yamada et al., 2012; Kalra et al., 2013), or head CT (Kilic et al., 2011; Korn et al., 2012; Ren et al., 2012).

## Image quality

Many parameters influence the quality of CT images. The goal of a clinical CT examination is to establish adequate image quality for a specific diagnostic task. Physical (objective) measures of image quality are often used for quality assurance and for optimisation of scanning settings to find minimum radiation exposure with no visible loss of detail. Image quality can be divided into three categories, low-contrast resolution, high-contrast resolution, and artifacts.

## Low-contrast resolution

Low-contrast resolution is the ability of the system to reproduce two adjacent objects with small differences in composition as separate structures, such as soft tissue with CT numbers close to each other with contrast differences between 4–10 HU. Low-contrast resolution or contrast-to-noise ratio (CNR) is a measure of the visibility of an object in an image. Determination of low contrast can be made by measurements in images of a phantom or by visual evaluation. Low-contrast phantoms often contain objects of different sizes and contrasts. The noise affects the low contrast, and the effect is greater with smaller objects. The level of low-contrast resolution is often given as percentage value, which represents the difference in CT number between the object and the background divided by the standard deviation (SD) of the background. Random noise is the statistical fluctuation in CT numbers and gives the image more or less noisy texture. If more photons are used (i.e., a higher dose), the closer each pixel value will be to the true value, and the SD of the pixel values will be less.

Generally, noise can be divided into three different types: quantum (stochastic) noise, system noise, and noise originating from the reconstruction process. In an ideal situation, the pixel value for water is zero. In reality, the pixel values vary around a mean value, and the variation (Poisson distributed) of this mean value is defined as the noise in the image, typically described by the SD of the pixel values (Verdun et al., 2015). Image noise shows the following relationship:

- $Noise = \frac{1}{\sqrt{mA}}$
- $Noise = \frac{1}{\sqrt{Rotation\ time}}$
- $Noise = \frac{1}{\sqrt{Slice\ thickness}}$

Quantum noise is inversely proportional to the square root of the absorbed dose to the detector (Hsieh, 2003). The same relationship is valid between rotation time and radiation dose. If the mAs (mA×rotation time) is doubled, the radiation dose is doubled. If the slice thickness is reduced by half, the tube current has to be doubled to obtain the same noise in the image. The more photons that contribute to the image, the closer the image will be to the real object.

The noise characteristics can be measured in the image by the noise power spectrum (NPS), which is described as a function of the spatial frequency, i.e., the noise distribution in the image (Verdun et al., 2015). Noise is the statistical fluctuation in CT numbers and is expressed as the SD of the mean CT number (HU) measured in a region of interest (ROI). Higher noise means more spread of the values. The image noise is often used to give an indication of whether or not the image quality is

sufficient. Using SD for direct comparison of noise levels between FBP and IR images is not valid because there may be a different distribution of the noise. To compare the noise distribution in CT images reconstructed with FBP and IR, it is more relevant to compare NPS of the images. NPS describes the characteristics of the noise and can be calculated from an ROI in a homogeneous phantom as:

$$NPS(u, v) = \frac{\Delta_x \Delta_y}{N_x N_y} (|FT[\Delta I(x, y)]|)^2 \quad (3)$$

where  $\Delta I$  is the deviation from the mean pixel value in a noise image and  $N_x$  and  $N_y$  are the number of pixels in the x and y directions (Verdun et al., 2015).

## High-contrast resolution

High-contrast resolution or spatial resolution is the ability of the system to resolve image details. The parameters that affect spatial resolution are limitations in the CT system like focal spot size, size of detector elements, slice thickness, pitch value, convolution filter, and pixel size. Selecting slice thickness is a balance between spatial resolution and noise because they counteract each other. Thinner slice thickness gives higher detail resolution but more noise. The spatial resolution affects visualisation of fine structures in, e.g., bone imaging, angiography, and lung. Spatial resolution can be expressed as the limiting resolution (i.e., the smallest resolvable object), or the modulation transfer function (MTF). Spatial resolution can be determined by several quantitative methods, such as scanning an image quality phantom including a wire or bar pattern and calculating the MTF (Droege et al., 1982; McNitt-Gray, 2006), or subjectively determining spatial resolution with a bar pattern.

## Image artifacts

Artifacts are structures appearing in the image that do not stem from the investigated object or patient. Artifacts in CT images can be considered as streaking, shading, rings, and distortions. These artifacts can be divided into four groups: physics-based, patient-based, scanner-based, helical/multi-section and aliasing artifacts (Hsieh, 2003).

- Physics-based artifacts result from the physical processes involved in the acquisition of CT data. Beam-hardening, photon starvation, and partial volume effect are some examples. Beam-hardening occurs when the X-ray beam passes through an object and lower energy photons are absorbed more easily than photons with higher energies. There are two types of artifacts that can appear from this effect: cupping and streaks between dense objects

in the image. Partial volume effect occurs when an object that is not centrally located in the CT slice is partially projected into the CT slice and causes shadow and streak artifacts. Photon starvation occurs in highly attenuating areas such as shoulders and appears as streaks and noise (Barrett et al., 2004).

- Patient-based artifacts are caused by patient movement and the presence of metal or other high-density material in or on the patient. Implants, dental fillings, and surgical clips in the scan field can lead to severe streaking artifacts (Barrett et al., 2004).
- Scanner-based artifacts, introduced by the detector, are often ring and distortion artifacts. The artifacts arise often when detector elements do not work properly (Barrett et al., 2004).
- Helical and multi-section artifacts are caused by the image reconstruction process. Stair-step artifacts appear around edges of structures in multi-planar and three-dimensional reformatted images when wide collimations and no overlapping reconstruction intervals are used. Zebra artifacts appear like faint stripes in multi-planar and three-dimensional reformatted images from helical data. The interpolation process gives rise to a degree of noise inhomogeneity along the z-axis (Barrett et al., 2004).
- Aliasing artifacts are caused by insufficient sampling frequency or undersampling of the image. If a too-large interval is used between projections, misregistration can appear. The artifacts occur as fine stripes looking like they radiate from the edge of a dense structure and appear a distance from the structure, also called “view aliasing”. Stripes close to the dense structure can also appear, which is called “ray aliasing” (Barrett et al., 2004).

## **Subjective evaluation of image quality**

Evaluation of patient images is the preferred way to assess the diagnostic quality of an image. Subjective evaluation of clinical examinations is recommended when evaluating the diagnostic use of an image. It is not easy to evaluate real clinical examinations to optimise examination protocols because it would not be appropriate to scan one patient several times. If a specific diagnosis is investigated, receiver operating characteristics (ROC) would be appropriate to use (Vining et al., 1992). ROC is an objective measurement that can be used to compare image techniques against human observer performance.

### *Visual grading characteristics*

Visual grading of the reproduction of important anatomical structures is one of many methods to determine the clinical image quality. The observers judge the image quality of different structures on a scale, e.g., from 0 to 4, where 0 is the lowest score (the anatomical structure is not visible) and 4 is the highest score (the structure is excellently reproduced). The rating data given by the observers in a visual grading study with multiple ratings is ordinal, meaning that non-parametric rank-invariant statistical methods are required. One method for determining the difference in image quality between two systems is called visual grading characteristics (VGC) analysis (Báth et al., 2007). The task of the observer is to rate his/her confidence about the fulfilment of image quality criteria. The criteria are typically based on European guidelines (European Commission, 2000), which provide guidance for selected CT examinations; the quality criteria presented define the level of performance considered necessary to produce images of diagnostic quality for a particular anatomical region. The rating data for the two systems are then analysed in a manner similar to that used in ROC analysis. The resulting measure of image quality is the VGC curve, which describes the proportions of the fulfilled image criteria. The area under the VGC curve is proposed as a single measure of the difference in image quality between two compared systems.

## Radiation dose and risks in CT imaging

The medical use of radiation must be justified; the principal aim of the medical exposures is to do more good than harm to the patient, in accordance with the ALARA principle (As Low As Reasonably Achievable). However, using too low radiation dose can result in poor image quality for a specific diagnostic task and in a worst-case scenario, make the examination useless and lead to an unnecessary radiation dose to the patient.

### **Radiation dose**

Many factors influence the radiation dose to the patient. A reduced radiation dose usually results in decreased image quality.

Information about the radiation dose is available after each CT examination. The CT dose index (CTDI) by volume (CTDI<sub>vol</sub>) and the dose length product (DLP) are automatically generated and displayed on the console.

The CTDI was first introduced for single-slice axial scanning and represented the average absorbed dose along the table feed direction (z-axis). The International

Electrotechnical Commission (IEC) has defined  $CTDI_{100}$  as the absorbed dose integrated over 100 mm for a single axial scan (IEC, 2009).  $CTDI_{100}$  refers to absorbed dose in air or in a cylindrical polymethyl methacrylate (PMMA) phantom representing the head (16 cm in diameter) and body (32 cm in diameter) with a length of 15 cm.  $CTDI_{100}$  is measured with a pencil ionisation chamber with a 100 mm active length:

$$CTDI_{100} = \int_{-50}^{+50} \frac{D(z)}{\min\{n \cdot T, 100 \text{ mm}\}} dz \quad (4)$$

where  $D(z)$  is the absorbed dose profile along the  $z$ -axis,  $n$  is the number of slices per rotation, and  $T$  is the nominal slice thickness.

To take account for the variations of the absorbed dose in the scan plane ( $x, y$ ), a weighted dose index ( $CTDI_w$ ) was introduced:

$$CTDI_w = \frac{1}{3} CTDI_{100(\text{central})} + \frac{2}{3} CTDI_{100(\text{peripheral})} \quad (5)$$

$CTDI$  by volume ( $CTDI_{vol}$ ) was introduced to take axial scan spacing into account:

$$CTDI_{vol} = \frac{CTDI_w}{pitch} \quad (6)$$

where  $pitch$  is the table transportation per rotation to the collimated beam width.  $CTDI_{vol}$  needs to be adjusted for patient size because it does not represent the average absorbed dose for objects with different size and shape (AAPM, 2011; AAPM, 2014).

For better representation of the overall energy delivered for the entire CT examination, the DLP was introduced. DLP is a measure of the total energy deposited in the phantom or patient:

$$DLP = CTDI_{vol} \cdot L \quad (7)$$

where  $L$  is the scan length.

## Radiation risk

When a person is exposed to ionising radiation, substantially two types of harmful effects can occur: stochastic and deterministic effects. The stochastic effects are dominated by cancer induction. There is also a risk for genetic damage, but this risk is less; it has never been possible to detect this genetic damage in humans, but laboratory tests on animals have shown such damage.

The effects of the ionising radiation depend on deoxyribonucleic acid (DNA) damage or damage to other parts of the cell nucleus. The deterministic effects arise when the radiation dose is higher than a certain threshold and gets more severe with higher radiation dose. The stochastic effects, also called late effects, consist primarily of induced cancer (Shah and Platt 2008). The probability that the effect will occur increases with increasing radiation dose.

The organs of the human body have different radiosensitivities, and this organ/tissue weighting factor ( $w_T$ ) has been addressed by the International Commission on Radiological Protection (ICRP) (ICRP, 2007b). The different sensitivities of the organs to ionising radiation and radiation type are taken into account when determining the effective dose (E). The weighting factor for radiation type ( $w_R$ ) is a relative factor reflecting the tendency of different types of radiation to cause cancer and genetic injuries. For X-rays, this weighting factor is 1. E is defined as follows:

$$E = \sum_T w_T H_T = \sum_T w_T \sum_R w_R D_{T,R} \quad (8)$$

where H is the equivalent dose, D is the absorbed dose, T is tissue, and R is radiation type. E is an indicator of stochastic risk.

Stochastic radiation effects are subject to a linear dose-response relationship with no absolutely safe lower threshold (LNT, linear no threshold hypothesis) (Little et al.; 2009).

Red bone marrow is one of the organs that is most sensitive to ionising radiation because of the immature stem cells that divide rapidly. Children have red bone marrow distributed throughout the skeleton up to the age of 5 years. The red bone marrow becomes more concentrated to the central skeleton with increasing age. Children have rapidly dividing cells and are more sensitive to the effects of radiation (Shah et al., 2008; Pearce et al., 2012; Mathews et al., 2013). Risk of cancer induction is significantly higher in children than in adults (Pierce et al., 2012). The latency period for leukaemia is around 5–7 years, and for solid carcinomas, it is 10–20 years or more. It is difficult to make individual risk assessments for particular patients and examinations. The concept of “effective dose” is defined by ICRP (ICRP, 1991; ICRP 2007b), and risk assessment should be done for populations rather than for individuals.

Rough estimates of the effective dose (E) for a CT examination can be obtained by multiplying DLP by a conversion coefficient (k) appropriate to the anatomical region that is examined. A detailed discussion on organ/tissue weighting factors for estimation of effective dose is provided in ICRP Publication 103 (ICRP, 2007b). The factors are useful for quick dose estimates and for large patient groups.

$$E = k \cdot DLP \quad (9)$$

# Aims

The overall aim of this thesis was to investigate and evaluate IR algorithms in terms of image quality and radiation dose, and in clinical practise to evaluate the potential of a new MBIR method for reconstructing paediatric abdominal CT examinations at a reduced radiation dose.

## Paper I

To evaluate the image quality produced by six different IR algorithms in four CT systems in the setting of brain CT, using different radiation dose levels and iterative image optimisation levels.

## Paper II

To investigate how image quality for abdominal CT depends on IR and MBIR and to discuss the potential for patient dose reduction.

## Paper III

To investigate the effect on image quality of reduced slice thickness combined with an MBIR method compared with standard slice thickness with IR for abdominal CT.

## Paper IV

To investigate whether MBIR could maintain or improve the image quality of paediatric abdominal CTs compared to the current IR method, when the radiation dose is reduced.



# Material and Methods

## Overview

This thesis includes two phantom studies (Papers I and III), one combined phantom/patient study (Paper II), and one patient study (Paper IV). The image quality phantom used was Catphan 600 (The Phantom Laboratory, Greenwich, NY, USA). Different modules for assessment of image quality available in Catphan 600 are shown in Figure 3.

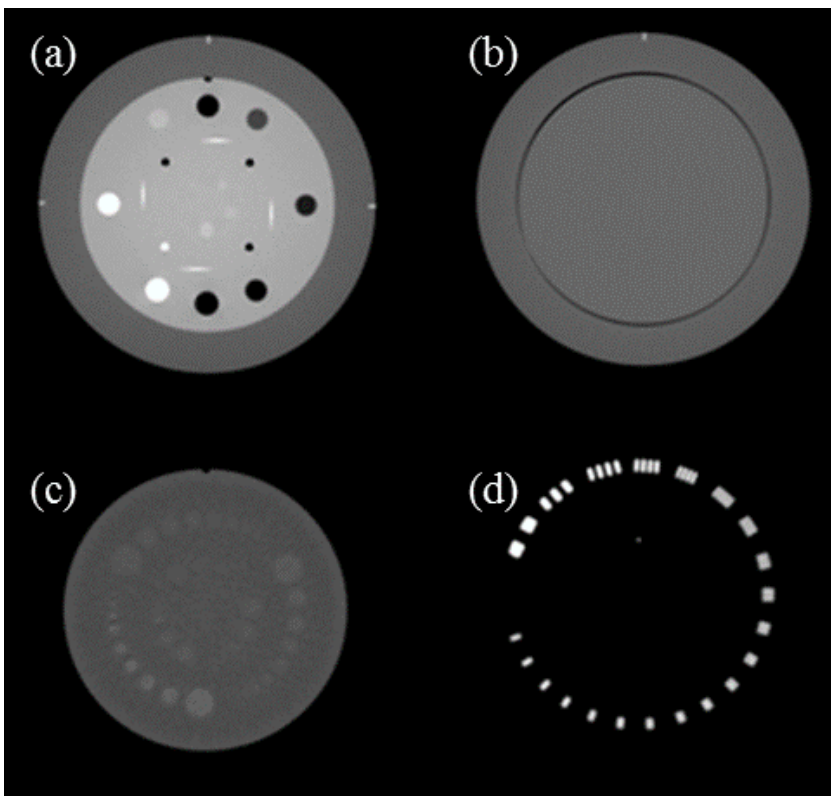


**Figure 3.** Image quality phantom Catphan 600® showing modules for assessment of CT numbers (a), noise and uniformity (b), low-contrast (c), and spatial resolution (d).

In Paper I, the image quality phantom was used with a Teflon ring to resemble skull bone (Teflon annulus CTP299, The Phantom Laboratory, Greenwich, NY, USA) to simulate the beam-hardening effects created by the skull in brain CT. In Papers II and III, the image quality phantom was used with and without a 25–35-cm oval body annulus (Oval annulus CTP579, The Phantom Laboratory, Greenwich, NY, USA). The annulus was used to better simulate the size and shape of a patient. Also in Papers II and III, an anthropomorphic torso phantom (CTU-41, Kyoto Kagaku Co., Ltd., Kyoto, Japan) was used for abdominal CT scans (Figure 4).

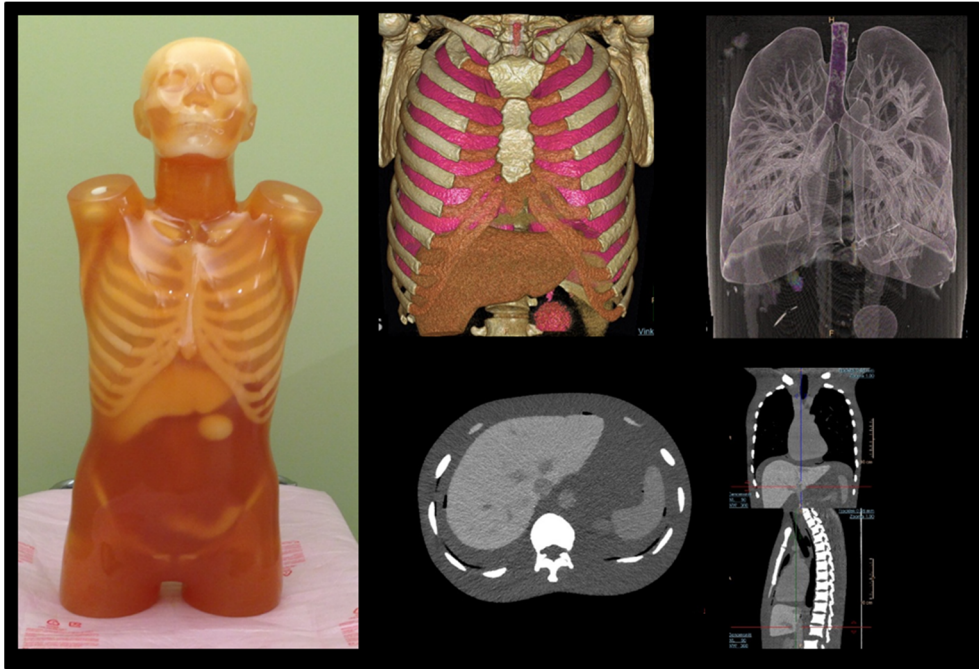


**Figure 4.** Anthropomorphic torso phantom, CTU-41, Kyoto Kagaku used for abdominal CT scans in Paper II and Paper III. Upper row showing CT images of the phantom, using volume rendered images of thorax/upper abdomen and pulmonary vessels/trachea. Lower row showing axial/coronal/sagittal images of the phantom.

Paper IV included 40 paediatric patients aged 1–15 years. They were all referred for an abdominal CT examination. An overview of the study subjects is presented in Table 2.

**Table 2.**

Overview of study subjects.

|  | Paper I      | Paper II     | Paper III    | Paper IV |
|--|--------------|--------------|--------------|----------|
| <b>Examined organ</b>                              | Brain        | Abdomen      | Abdomen      | Abdomen  |
| <b>Image quality phantom</b>                       | Yes          | Yes          | Yes          | -        |
| <b>Accessories used with image quality phantom</b> | Bone annulus | Body annulus | Body annulus | -        |
| <b>Antropomorphic phantom</b>                      | -            | Yes          | Yes          | -        |
| <b>Patient</b>                                     | -            | -            | Yes          | Yes      |

## Scanning technique

In Paper I, the reference radiation dose was adjusted according to the European guidelines on quality criteria for CT (European Commission, 2000), and other examination parameters were chosen according to recommendations for adult brain CT published by the American Association of Physicists in Medicine (AAPM), (AAPM, 2012).

In Paper II, the reference radiation dose was chosen to match the diagnostic reference level for an abdominal CT examination (SSM, 2009), the 10 mGy dose level was chosen to match the clinical protocol used in the authors' institution, and the lowest dose level was chosen to match a low-dose protocol. The anthropomorphic phantom was scanned with a standard protocol for CT abdomen used at the authors' institution, which was chosen as the reference radiation dose. The mA was lowered by 50%, which resulted in a  $CTDI_{vol}$  of 3.6 mGy. The third scan on the anthropomorphic phantom was a low-dose protocol at 100 kV and 57 mAs, which resulted in  $CTDI_{vol}$  of 2.3 mGy.

The scanning parameters used in Paper III were from a standard CT abdomen protocol used at the authors' institute.

In Paper IV, the reference radiation dose refers to a protocol used at the authors' institution, a standard protocol for paediatric CT abdomen for paediatric patients between 11 and 50 kg.

An overview of the scanning techniques used in Papers I–IV is presented on next page (Table 3).

**Table 3.**

Scan parameters used in Papers I–IV.

|   | Paper I  | <sup>1</sup> Paper II                            |                                      | <sup>2</sup> Paper III |                            | Paper IV  |
|---|--|--|--------------------------------------|------------------------|----------------------------|---|
| <b>Vendor</b>                               | GE, Philips, Siemens, Toshiba                  | Philips  |                                      | Philips                |                            | Philips   |
| <b>Tube voltage (kV)</b>                    | 120  | 80, 100, 120, 140                                | 100, 120                             | 120                    |                            | 100   |
| <b>Dose modulation</b>                      | Disabled                                       | Disabled   | <sup>3</sup> ACS and Z-DOM           | Disabled               | <sup>3</sup> ACS and Z-DOM | <sup>4</sup> 3D modulation  |
| <b>Tube load (mAs)</b>                      | Variable                                       | Variable   |                                      | Variable               |                            | Variable  |
| <b><sup>5</sup>CTDI<sub>vol</sub> (mGy)</b> | 120 (100%)<br>84 (70%)<br>48 (40%)<br>12 (10%) | 25 (100%)<br>17.5 (70%)<br>10 (40%)<br>2.5 (10%) | 7.1 (100%)<br>3.6 (50%)<br>2.3 (30%) | 10                     | 7.1                        | <sup>6</sup> 2.7 (1.4–4.2) (standard)<br><sup>6</sup> 1.9 (1.2–3.5) (low) |
| <b>Detector configuration</b>               | Variable                                       | 128×0.625  |                                      | 128×0.625              |                            | 64×0.625  |
| <b>Pitch</b>                                | Variable                                       | 0.6  | 0.993                                | 0.6                    | 0.993                      | 1.2   |

<sup>1</sup>Paper II, left column shows the scanning parameters for Catphan 600 and right column for the anthropomorphic phantom.

<sup>2</sup>Paper III, left column shows scanning parameter for Catphan 600 and right column for the anthropomorphic phantom.

<sup>3</sup>Philips dose-modulation system Dose Right, automatic current selection (ACS) and longitudinal modulation Z-DOM.

<sup>4</sup>Philips dose modulation system Dose Right, 3D modulation.

<sup>5</sup>CTDI<sub>vol</sub> corresponds to 16 cm phantom in Paper I and 32 cm phantom in Papers II–IV.

<sup>6</sup>The CTDI<sub>vol</sub> are given as median and (range).

## Image reconstruction

FBP was used as a baseline in Papers I, II, and III. In Paper I, three levels of IR were used, corresponding to low-, medium-, and high level of IR, and for the MBIR, one level were used. An overview of levels used in Paper I is shown in Table 4.

**Table 4.**

IR and MBIR level used in Paper I. IR level was chosen to reflect the complete range of available levels: low (IR Level 1), medium (IR Level 2), and high (IR Level 3).

| Vendor CT system  | GE Discovery CT 750HD | Philips Brilliance iCT     | Siemens Definition Flash | Toshiba Aquilion One |
|-------------------|-----------------------|----------------------------|--------------------------|----------------------|
| <b>Standard</b>   | FBP                   | FBP                        | FBP                      | FBP                  |
| <b>IR Level 1</b> | ASIR 10%              | iDose <sup>4</sup> level 1 | SAFIRE strength 1        | AIDR 3D mild         |
| <b>IR level 2</b> | ASIR 50%              | iDose <sup>4</sup> level 3 | SAFIRE strength 3        | AIDR 3D standard     |
| <b>IR level 3</b> | ASIR 90%              | iDose <sup>4</sup> level 5 | SAFIRE strength 5        | AIDR 3D strong       |
| <b>MBIR</b>       | Veo                   | IMR low-contrast L2        | N/A                      | N/A                  |

In Papers II and III, FBP, IR, and MBIR on a Philips system were evaluated with different levels of IR and MBIR to cover the whole range of available levels. FBP was used as a baseline.

In Paper IV, the standard setting of Philips IR (iDose<sup>4</sup>) was used as baseline, which is the standard setting for paediatric CT abdomen at the authors' institution. One level of Philips MBIR (IMR) and the standard setting of Philips IR (iDose<sup>4</sup>) were used for the low dose examination.

An overview of all image reconstructions used in Papers I–IV is shown in Table 5.

**Table 5.**  
Image reconstructions.

|                             | Paper I                                    |     | Paper II           | Paper III          | Paper IV           |
|-----------------------------|--|-----|--------------------|--------------------|--------------------|
| <b>Slice thickness (mm)</b> | 5  |     | 1, 3, 5            | 1, 3, 5            | 0.9, 5             |
| <b>FBP</b>                  | Yes  |     | Yes                | Yes                | No                 |
| <b>IR</b>                   | ASiR, iDose <sup>4</sup> , SAFIRE, AIDR 3D |     | iDose <sup>4</sup> | iDose <sup>4</sup> | iDose <sup>4</sup> |
| <b>IR level</b>             | 1, 2, 3                                    |     | 1, 3, 5            | 1, 3, 5            | 4                  |
| <b>MBIR</b>                 | Veo  | IMR | IMR                | IMR                | IMR                |
| <b>MBIR level</b>           | -  | 2   | 1, 2, 3            | 1, 2, 3            | 1                  |

<sup>1</sup> IR level used in Paper I is shown in detail in Table 4.

## Image quality assessment

By studying phantoms, an indication was achieved about the change in image appearance for patients, and in addition, information was obtained about how much it would be possible to lower the radiation dose without compromising image quality. Image quality phantoms were used to evaluate and assess image quality parameters, and to obtain a more patient-like image quality phantom, body and ring annulus were used. A further step to a more patient-like situation, was the use of an anthropomorphic phantom.

In Papers I–III, phantoms were used to evaluate both objective and subjective assessments of image quality. In Paper IV, objective measurement in liver was performed, and VGC analysis was performed. Objective image quality parameters were chosen to include information on noise and high- and low-contrast resolution. Subjective evaluation was based on clinically important structures. Table 6 shows an overview of image quality aspects used in the different papers.

**Table 6.**  
Image quality assessment.

|                            | Paper I | Paper II | Paper III | Paper IV |
|----------------------------|---------|----------|-----------|----------|
| <b>Objective</b>           |         |          |           |          |
| Noise                      | ✓       | ✓        | ✓         | ✓        |
| CT number                  | ✓       | ✓        |           |          |
| SNR                        | ✓       | ✓        |           |          |
| CNR                        | ✓       | ✓        | ✓         |          |
| NPS                        | ✓       | ✓        |           |          |
| MTF                        | ✓       | ✓        |           |          |
| <b>Subjective</b>          |         |          |           |          |
| Number of observers        | 5       | 3        | 3         | 3        |
| Low-contrast               | ✓       | ✓        | ✓         |          |
| Spatial resolution         |         | ✓        |           |          |
| Anatomical structures      |         |          |           | ✓        |
| Number of quality criteria | 2       | 2        | 2         | 7        |

For the objective assessment of phantom images for Catphan 600, the program Auto QA Lite™ (v3.01, 2010, Iris QA, LLC, Frederick, MD, USA) was used for automatic evaluation of image quality parameters. Assessment of CT number, noise, uniformity, and spatial resolution was made using the different phantom modules. CT numbers were measured for seven different materials. In the image uniformity module, the mean attenuation (HU) and noise (SD) were calculated. Five identical ROIs were placed on the image of the uniformity module, four peripherally and one centrally. The uniformity was defined as the maximum difference in CT number between the central ROI and the peripheral ROIs. Noise was determined using the measurements from all five ROIs.

Calculation of NPS (equation 3) was made using the image processing program ImageJ (v1.46, National Institute of Health, Bethesda, USA) and the plugin Radial Profile Plot (by Paul Baggethun, version 2009/05/14) in reconstructed images of the uniformity module of Catphan 600.

Low-contrast resolution was assessed using the low-contrast module of the phantom. The module contains three sets of outer supra-slice cylinders with nominal contrasts of 1.0% (10 HU), 0.5% (5 HU), and 0.3% (3 HU). Each set consists of nine cylinders with diameters from 2 to 15 mm.

CNR was calculated using the following equation:

$$CNR = \frac{|HU_{Object} - HU_{Background}|}{SD_{Background}} \quad (9)$$

where the CT numbers (HU) and noise (SD) were measured in the low-contrast module in identical ROIs placed in the largest cylinder in each of the three sets, as well as in the background.

In the subjective evaluations of image quality, a Java-based image evaluation program ViewDex (Viewer for Digital Evaluation of X-ray images) (Håkansson et al., 2010) was used to view and record the ratings. The program displayed the images in a random order and all annotations, information on dose level, and type of reconstruction were hidden. All subjective evaluations were done on a PACS (Picture Archiving and Communication System) station with a proper reading environment. In the clinical study, the radiologists (three paediatric radiologists, 19–26 years of experience in diagnostic radiology and 13–21 years in paediatric radiology) were free to adjust window level/width to simulate standard clinical reading process.

The subjective evaluation of low-contrast resolution in the phantom studies was done in consensus by five observers in Paper I, two medical physicists and three radiologists with 5–22 years' experience, and three observers in Papers II and III (medical physicists with 7–12 years of experience of reading CT imaging), respectively, using two criteria:

- Smallest discernible cylinder
- Smallest sharply defined cylinder

In Paper IV, a 4-point grading scale was used to rate how well five anatomical structures (liver parenchyma and intrahepatic vessels, pancreatic contours, aorta, adrenal glands, spleen) were reproduced. The following scale was used:

- N/A: Not Applicable
- Grade 1: Not at all
- Grade 2: Poorly
- Grade 3: Acceptably
- Grade 4: Clearly

After the five questions about visualisation of the anatomical structures, the radiologists were asked two questions about how they perceived the general image quality. The rating scale used for the evaluation was as follows:

- Grade 1: Unacceptable
- Grade 2: Poor
- Grade 3: Sufficient
- Grade 4: Excellent

A program for analysing VGC data called “VGC Analyzer” (Båth and Hansson 2016) was used. VGC analysis is a non-parametric rank variant method for analysis of visual grading data (Båth et al., 2007). Image quality is rated for two different reconstruction methods or radiation levels and compared by producing VGC curve. VGC Analyzer determines the area under the VGC curve and its uncertainty using non-parametric resampling techniques. The software is made for statistical analysis of fully crossed, multiple-reader, multi-case VGC studies. VGC Analyzer is a software written in IDL (Research System, Inc, Boulder, CO, USA). The program produces statistical analysis of the rating data from studies performed with multiple readers and multiple cases, and all readers grade/assess all cases. Determination of the area under the curve (AUC) for the VGC study and non-parametric methods are applied for the statistical tests, and a bootstrapping resampling technique and a permutation resampling technique are used to determine the confidence interval (CI) and the p-value for testing null hypothesis. If the two compared methods are equal, the  $AUC_{VGC}$  will be 0.5.

An intraclass correlation coefficient (ICC) was used for assessing the inter-observer variability of rating the same criteria by three observers. ICC with 95% CI was calculated with SPSS Statistics (Statistical Package for the Social Science, IBM, Armonk, NY, USA) using a two-way mixed model. Intra-observer variability was evaluated on duplicated cases and defined as the number of equivalent ratings for the first and second evaluations for the specific observer.

# Results and discussion

This thesis involved investigating the effects of using more advanced reconstruction methods on image quality and radiation dose to patients for CT examinations. All studies showed that the radiation dose can be reduced with new reconstruction methods while keeping or in some cases even improving image quality.

## Image quality

One aim of this thesis was to investigate how IR and MBIR affect image quality. The biggest concern with new image processing is that it would change something in the image that would leave a false impression or remove structures. FBP was used as baseline in Papers I and II and was compared to different settings of IR and MBIR in combination with different radiation doses.

### **Noise and spatial resolution**

Image quality improvement such as reduction of noise is a prerequisite for acceptance of lowering the radiation dose. The noise is the most discussed image quality parameter when it comes to IR. Other important parameters are low-contrast resolution and spatial resolution. The results from the objective measurements of noise (SD) and spatial resolution in Paper I are shown as percentages relative to FBP in Table 7. All IR reduced noise, and for Philips and GE, also maintained the spatial resolution (MTF), but for both Siemens and Toshiba a slightly decreased spatial resolution was observed. Philips MBIR (IMR) and GE MBIR (Veo) also proved to be the most effective in lowering the noise at a reduced radiation dose. According to the vendor, GE MBIR (Veo) allows better spatial resolution than GE IR (ASIR) and FBP (Thibault, 2010). Studies also reported on GE MBIR (Veo) found substantial decrease in image noise and increase in CNR compared to GE IR (ASIR) and FBP (Scheffel et al., 2012).

**Table 7.**

Comparison of noise and resolution for different doses and different CT systems. The percent change in noise (SD) and spatial resolution (MTF<sub>10%</sub>) is presented compared to FBP. The values marked in green indicate improvement with IR/MBIR of more than 5%, and values marked in red indicate impairment of more than 5%. The best result for each CT system and radiation dose, respectively, is indicated in bold.

|                | 12 mGy    |                    | 48 mGy    |                    | 84 mGy    |                    | 120 mGy   |                    |
|----------------|-----------|--------------------|-----------|--------------------|-----------|--------------------|-----------|--------------------|
|                | Noise     | MTF <sub>10%</sub> |
| <b>GE</b>      |           |                    |           |                    |           |                    |           |                    |
| FBP            | 100       | 100                | 100       | 100                | 100       | 100                | 100       | 100                |
| IR1            | 94        | 101                | 89        | 101                | 87        | 101                | 86        | 100                |
| IR2            | 68        | 104                | 66        | 104                | 63        | 104                | 62        | 103                |
| IR3            | <b>46</b> | 108                | <b>46</b> | 107                | <b>43</b> | 106                | <b>42</b> | 106                |
| Veo            | 67        | <b>134</b>         | 89        | <b>149</b>         | 98        | <b>141</b>         | 97        | <b>136</b>         |
| <b>Philips</b> |           |                    |           |                    |           |                    |           |                    |
| FBP            | 100       | 100                | 100       | 100                | 100       | 100                | 100       | 100                |
| IR1            | 88        | 100                | 91        | 102                | 94        | 100                | 97        | 100                |
| IR2            | 77        | 100                | 80        | 102                | 77        | 100                | 79        | 101                |
| IR3            | 64        | 102                | 67        | 102                | 63        | 100                | 66        | 97                 |
| IMR            | <b>44</b> | <b>113</b>         | <b>52</b> | <b>117</b>         | <b>59</b> | <b>117</b>         | 69        | <b>119</b>         |
| <b>Siemens</b> |           |                    |           |                    |           |                    |           |                    |
| FBP            | 100       | 100                | 100       | 100                | 100       | 100                | 100       | 100                |
| IR1            | 83        | 90                 | 87        | 93                 | 85        | 87                 | 85        | 88                 |
| IR2            | 67        | 87                 | 74        | 92                 | 71        | 89                 | 71        | 87                 |
| IR3            | <b>53</b> | 86                 | <b>60</b> | 91                 | <b>58</b> | 89                 | <b>59</b> | 88                 |
| <b>Toshiba</b> |           |                    |           |                    |           |                    |           |                    |
| FBP            | 100       | 100                | 100       | 100                | 100       | 100                | 100       | 100                |
| IR1            | 65        | 73                 | 78        | 83                 | 77        | 95                 | 77        | 93                 |
| IR2            | 57        | 72                 | 62        | 84                 | 66        | 95                 | <b>66</b> | 95                 |
| IR3            | <b>54</b> | 67                 | <b>58</b> | 81                 | <b>61</b> | 91                 | 67        | 94                 |

Philips IR (iDose<sup>4</sup>) did not affect the spatial resolution compared to FBP. The resolution can be improved if a sharper filter is used in combination with Philips IR, which was demonstrated in a previous study (Olsson et al., 2012). In our institution, a standard protocol with Philips IR is routinely used with a sharper kernel, for example, for standard CT abdomen, Philips IR level 4 and filter C are used.

Previous studies on Philips IR (iDose<sup>4</sup>) (Funama et al., 2011; Noel et al., 2011; Habets et al., 2012; Utsunomiya et al., 2012) have shown reduced noise and increased CNR compared to FBP at standard dose CT. Low-dose CT examinations reconstructed with Philips IR (iDose<sup>4</sup>) have shown similar image quality compared to standard dose reconstructed with FBP.

### **Low-contrast resolution**

The low-contrast resolution is a very important parameter, e.g., in liver and brain examinations. To reach an acceptable level of the low-contrast resolution in brain and liver, normally a high radiation dose is required. The image quality phantom gives an indication of how the image quality is affected by IR and MBIR. Subjective assessment of the low-contrast resolution showed that the object visibility increased with increased radiation dose.

In Paper II, the results showed that in images reconstructed with Philips MBIR (IMR), the low-contrast objects were reproduced as defined objects more discernibly and sharply than Philips IR (iDose<sup>4</sup>) for the same dose level. The visibility of objects increased with increasing level of radiation dose up to 17.5 mGy. At higher dose levels, no further improvement was achieved.

The main clinical improvement with IMR is the noise reduction and the improvement in low-contrast resolution in liver and abdominal scans (Park et al., 2016), where low-contrast resolution is needed.

### **Slice thickness**

The results from Paper III showed that it is possible to use reduced slice thickness with Philips MBIR (IMR) compared to Philips IR (iDose<sup>4</sup>). Enhanced low-contrast and effective noise reduction make it possible to use reduced slice thicknesses when reading CT images reconstructed with IMR. The higher the level of IMR, the less important the slice thickness. With thinner slices, the effect of partial volume artifacts is also reduced. The results from noise measurements in the liver for the anthropomorphic phantom are shown in Figure 5. The anthropomorphic phantom was scanned with different dose levels, and the images were reconstructed with FBP, IR levels 1–3, and MBIR levels 1–3 and in combination with different slice

thicknesses. The highest level of IR with a 5-mm slice width resulted in images with more noise compared to the lowest level of IMR and 1-mm slice width.

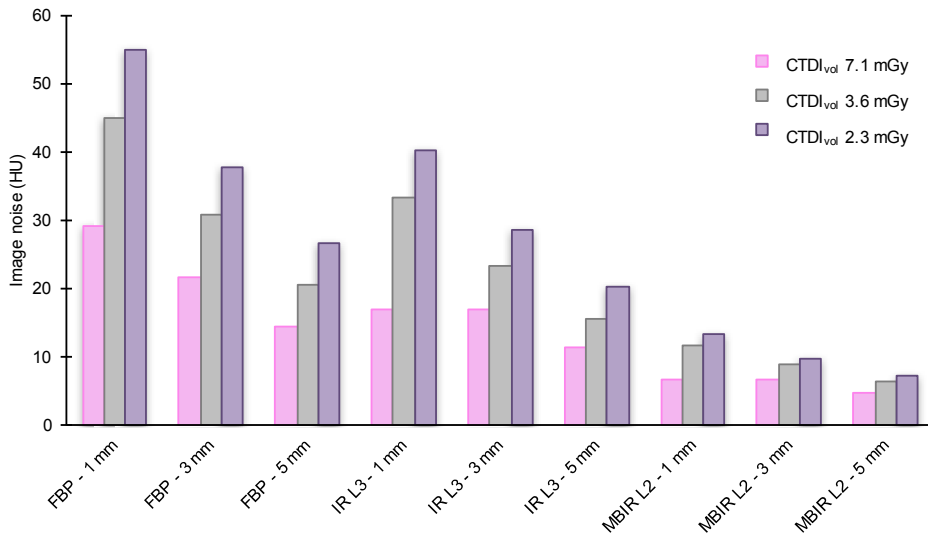


**Figure 5.** Image noise measured in the liver for an antropomorphic phantom for different radiation dose levels (CTDI<sub>vol</sub> 7.1, 3.6 and 2.3 mGy) and different image reconstructions (FBP, Philips IR L3 (iDose<sup>4</sup> levels 3) and Philips MBIR L2 (IMR levels 2) for different slice thicknesses (1, 3, and 5 mm).

## Noise power spectrum

The NPS is a useful metric for understanding the noise content in images. Measurement of image noise in the form of variation in the pixel values (SD is the most commonly used) is available and easy to perform at an ordinary workstation. But the measurement of the SD may not fully reflect the impact that the noise will have on a diagnostic task. If a smoothing filter is used, it will affect the noise but not the information content in the image. The NPS describes the magnitude of the noise at each spatial frequency. In this thesis, NPS was measured in two dimensions, which focuses on characterising the noise correlation and noise magnitude in the axial images.

The noise for FBP follows the classical power law:

$$Noise_{FBP} = \frac{1}{\sqrt{mA}} = (mA)^{-0.5} \quad (10)$$

In other published studies (Li et al., 2014), MBIR is claimed to follow the below power law:

$$Noise_{MBIR} \approx (mA)^{-0.25} \quad (11)$$

The shape of the NPS curve illustrates the characteristics of the image noise, and the amplitude of the curve is related to the amount of noise (Li et al., 2014). The NPS curve for the Philips system, with FBP, IR (iDose<sup>4</sup>), and MBIR (IMR), showed similar shapes of the NPS curve for FBP and iDose<sup>4</sup>. The amplitude for the NPS of Philips IR (iDose<sup>4</sup>) was lower than for FBP, which demonstrates the noise reduction. The amplitude of the NPS curve decreases with higher levels of Philips IR (iDose<sup>4</sup>). For Philips MBIR (IMR), the NPS curve differs in shape and amplitude compared to FBP and IR (iDose<sup>4</sup>). The NPS curve calculated from Catphan images is shown in Figure 6.

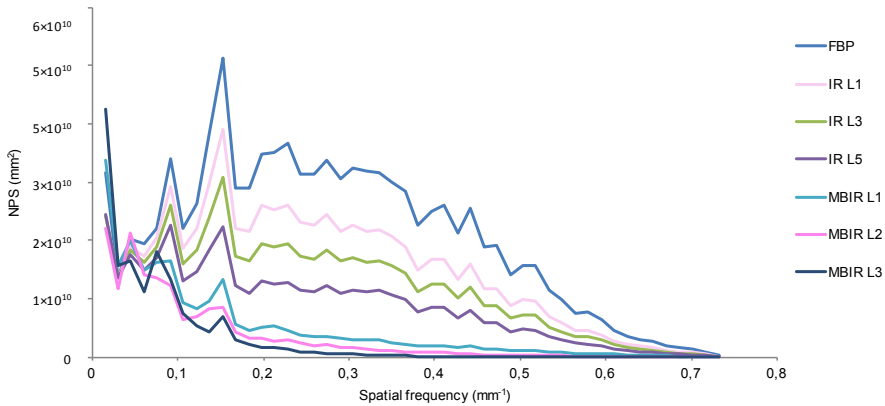


**Figure 6.**

Noise power spectra (NPS) after scanning the Catphan phantom with body annulus at 120 kV and 10 mGy and reconstructing the images with filtered back projection (FBP), iDose<sup>4</sup> levels 1, 3, 5 (IR L1, L3, L5) and IMR levels 1–3 (MBIR L1–L3). The curve form represents the distribution of noise (y-axis) as a function of spatial frequency (x-axis). Higher amplitude of the curves imply more noise.

This results supports the common opinion among radiologists that images reconstructed with Philips MBIR (IMR) have an unnatural and unfamiliar expression. With increased noise reduction, the NPS shift is more pronounced, which may affect the level of noise reduction. The images become smoother and appear more like a picture made with watercolours (Figure 7).

Paper I showed that the NPS curves had the greatest downward shift between FBP and IR for GE. The shape of the NPS curve was most consistent between FBP and IR for the Philips system. Other studies on Philips IR (iDose<sup>4</sup>) reported no difference in image texture compared to FBP (Funama et al., 2011; Habets et al., 2012), which also is shown in Figure 6. The most pronounced differences with respect to amplitude and shape of the NPS curves were between the MBIR algorithms and FBP.

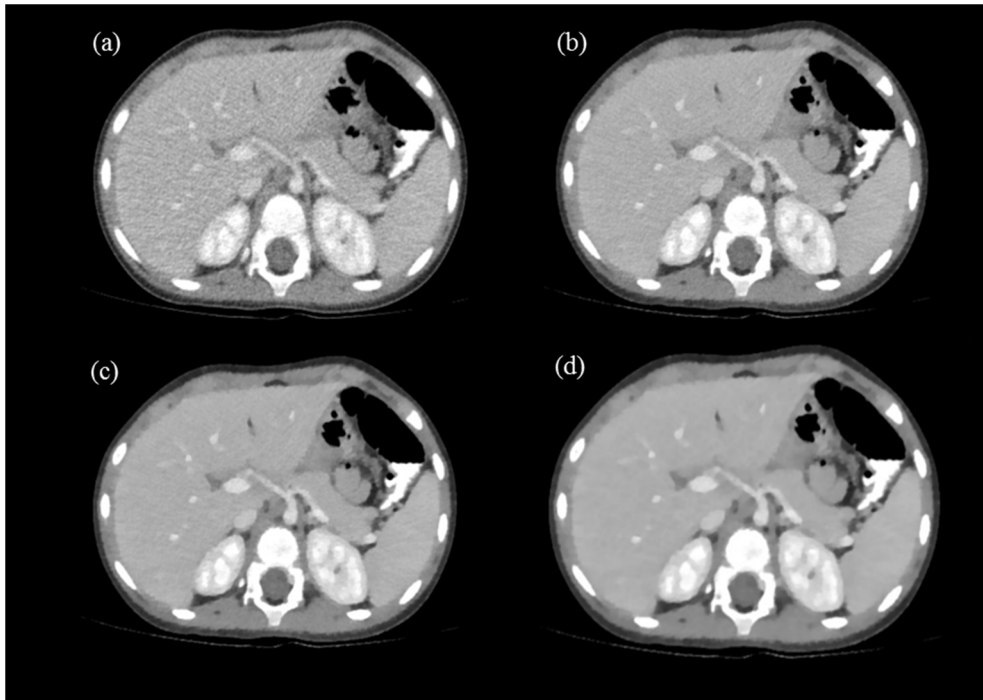


**Figure 7.** CT abdomen on a 4-year-old female patient scanned with 32% lower radiation dose. Image reconstructed with Philips IR (iDose4 L4) and three levels of Philips MBIR (a), IMR L1 (b), IMR L2 (c), and IMR L3 (d). CT images may not be adequately produced in print.

## CT numbers

There is a difference in absolute CT numbers for specific materials among different CT systems. The largest deviation was found for Teflon, radiation dose 12 mGy, measuring CT numbers between 903 to 1100 HU for the different vendors. However, within each CT system, the difference between FBP and IR was in most cases negligible ( $\leq 4$  HU) (Paper I).

In Paper II, the CT numbers were also investigated, but in this paper, all tube voltage steps were included for different radiation dose levels and for FBP, Philips IR (L1, L3, L5), and Philips MBIR (L1, L2, L3). The results showed that the CT numbers were stable among the FBP, Philips IR (iDose<sup>4</sup>), and Philips MBIR (IMR). The differences between the different reconstruction methods were of the same order for all tube voltages. It is well known that the tube voltage affects the absolute CT numbers, which was also noted. For this study as well, it turned out that Teflon measured the largest deviation. A study performed by Dodge et. al., also showed that the CT numbers in GE MBIR are highly sensitive to low-dose levels especially for materials above 200 HU (Dodge et. al., 2016).

It is important to point out that the CT numbers depend on tube voltage and filtration and that the CT numbers is calibrated for each CT system individually.

## **Artifacts**

The impact of IR on image artifacts is not within the scope of this thesis. Some published data indicate no difference in artifacts between IR with low dose and FBP with normal dose (Prakash et al., 2010; Sagara et al., 2010). However, some studies have reported reduced streak artifacts using Philips IR (iDose<sup>4</sup>) (Funama et al., 2011; Habets et al., 2012; Oda et al., 2014) and Philips MBIR (IMR) (Oda et al., 2014).

One study found increased severe artifacts using GE IR (ASIR) in pulmonary CT (Honda et al., 2011). An explanation can be that the high CT number from streak artifact was recognised as an anatomic structure and enhanced after IR.

## **Radiation dose**

One important aim of this thesis was to evaluate the potential of IR algorithms to reduce radiation dose and in particular the new Philips MBIR (IMR) for paediatric abdominal CT, compared to current reconstruction methods. Indications for introducing IR are mainly that low radiation doses are required and that there is a need for a good low contrast in the images. The principal aim of the medical exposures in general is to do more good than harm, in accordance with the ALARA principle.

Drawing conclusions about how much it is possible to reduce the radiation dose when using IR methods requires a great deal of knowledge about how image quality is affected, and how accepted the “new” images will be in the clinic. One must bear in mind that reported dose reductions are relative to the original dose level, i.e. an

examination which originally has a high radiation dose has potential for a large dose reduction (even without implementing iterative reconstruction!).

The image quality in paediatric imaging was evaluated after a 32% dose reduction and introduction of IMR (Paper IV). The original scan protocols were optimised with IR, and in this study, the dose reduction was limited to one third of the original dose as a first step. This choice might be considered as a moderate dose reduction in comparison to the phantom studies. The risk of lowering the radiation dose too much is that the images will not be proper for diagnostic purposes. The radiologists who evaluated these images have long experience in paediatric radiology (13–21 years) and are used to “noisy” images. They also had previous experience with IMR. The VGC analysis compared the standard protocol, Philips IR (iDose<sup>4</sup>), with Philips MBIR (IMR) with 32% lower radiation dose. The result showed no difference between the two techniques, which was expected. If the clinical protocols already are optimised according to ALARA, the main reason for introducing IR and MBIR is to lower the radiation dose and keep the image quality unchanged or improved.

Many studies have dealt with the clinical use of IR, both with subjective and objective measurement of image quality. The conclusions were that image quality was maintained or improved without diagnostic compromise compared to older techniques (Shuman et al., 2013; Bahn et al., 2015; Gandhi et al., 2016). However, radiologists do need time to work with IR images to become accustomed to the different look and gain confidence in the diagnostic capability. Typically, after about 90 days, many radiologists hardly notice the difference in the image appearance (Shuman, 2016). Some studies have found, however, that aggressive dose reduction can reduce lesion detection even with MBIR (Pickhardt et al., 2012; Jensen et al., 2014). Each manufacturer offers several types of IR (Table 1), sometimes depending on the model of the scanner. It is important to optimise the CT protocols based on the clinical issue and to use the IR and MBIR to achieve the lowest possible radiation dose without jeopardising the diagnostic outcome.

## Clinical implementation

The following changes have been made in the author’s institution after investigations included in this thesis.

Paper I was used as a basis for clinical diagnostic acceptability studies that aimed for further dose reduction and retention of image quality (Löve et al., 2014). A dose reduction of 30% was implemented for brain CT and the images reconstructed with Philips IR (iDose<sup>4</sup>) with level 2. These are now the standard settings for adult brain CT for all Philips CTs at the authors’ institution.

Paper II was also used as a basis for clinical diagnostic acceptability studies, such as Paper IV. A poster at the European Congress of Radiology, Vienna, 2014, (Olsson et al., 2013), showed the improvement of CT image quality with Philips IR. In this study, a sharper kernel was used with Philips IR to improve the spatial resolution. After this study, a standard protocol with Philips IR has been routinely used with a sharper kernel in our institute; for example, standard CT abdomen investigations are done with Philips IR level 4 and filter C.

In Paper III, it was shown that images reconstructed with Philips MBIR (IMR) and thinner slices can be used without degrading image quality. All images that are reconstructed with Philips MBIR are routinely viewed at 0.9 mm slice thickness.

Paper IV showed that a 32% dose reduction for paediatric abdominal CT examination reconstructed with Philips MBIR, level 1, did not degrade image quality. The implementation of this method has already been achieved at the authors' institution.

## Summary of results

The following results are shown in this thesis:

- The different IR algorithms have different strengths and weaknesses, but the important conclusion is that all vendors have improved most or all image quality parameters compared to FBP.
- For all IR algorithms, subjective image quality was improved. Noise, SNR, and CNR were all improved, although to a variable degree.
- Spatial resolution was improved only for MBIR algorithms and for GE IR (ASIR).
- The IR algorithms improved image quality irrespective of radiation dose.
- The MBIR algorithms improved image quality progressively with decreasing radiation dose.
- The MBIR algorithms affected image appearance, which can be attributed to the NPS.
- With Philips MBIR (IMR), it is possible to use thinner slices and maintain or even improve image quality.
- With Philips MBIR (IMR), it is possible to reduce the radiation dose and improve low-contrast resolution for low-contrast scanning such as brain and abdominal scans.

- A 32% dose reduction with Philips MBIR (IMR) in paediatric abdominal CT is possible without degradation of image quality.

# Conclusion

The radiation dose can be reduced with new IR methods while maintaining or in some cases even improving image quality compared to older reconstruction methods.

## Future aspects of this research field

FBP has been the standard of image reconstruction in CT. However, the FBP method reconstructs noisy images with possible artifacts when the radiation dose is reduced considerably. IR has replaced FBP more and more in recent years and has shown good potential for replacing it completely, especially when performing low-dose examinations. Today, most IR methods are mainly based on denoising of the images. Knowledge and model-based IR will certainly develop in line with computer capacity as it increases. It is important that these knowledge-based and fully model-based IR techniques can reconstruct images in a timely manner that is acceptable in the clinic. These advanced model-based reconstruction methods applied to ultra-low-dose CT might replace some conventional radiographic examinations, which might cause some concern for radiologists because it will generate significantly more images.

An ongoing study includes paediatric CT examinations with the aim to evaluate how much the radiation dose can be reduced. In collaboration with Philips, a noise-simulation tool is used to simulate CT scans acquired with lower radiation doses. The study will include paediatric patients from 0 to 12 years of age and CT examinations of brain, thorax, and abdomen. It would also be interesting to further investigate other vendors of IR and MBIR and include artifacts that are an important area of image quality.

Multi-professional collaboration will be necessary to fully assess different scan parameter settings, image reconstruction and kernel combinations, and optimisation of contrast medium to achieve adequate CT examinations with the lowest possible radiation dose. This type of collaboration must also involve the vendors in the form of application and product specialists. Everyone works for the united goal of achieving the ALARA principle in diagnostic radiology.



# Acknowledgements

First of all, I would like to thank my former supervisor and former head of the Medical Physics department in Malmö, Sören Mattsson for giving me the opportunity for making this thesis possible. I would also like to thank Mats Nilsson for supporting Sören in his decision to allow me to do my doctoral graduation despite my position as a medical physicist. Your knowledge, good advice and criticism of this thesis has been appreciated.

Next I would like to express my sincere gratitude to my supervisor Marcus Söderberg, Kristina Ydström and Anders Tingberg. Marcus for always be available and get things done right away. Thanks for sharing your knowledge and always being open for discussions. Kristina, my friend, roommate and supervisor, we share so many interests both within research but also outside work. Anders, for your interest in supporting my academic efforts and giving me the opportunity to focus on this project. Thank you for valuable discussions.

Furthermore, I would like to thank my co-authors on the papers included in this thesis: Fredrik Stålhammar, Askell Löve, Kristina Stayer von Schultz, Roger Siemund, and Isabella Björkman Burtscher, it has been a pleasure working with you. Especially thanks to Fredrik, Kristina and Pär Wingren for your effort to review all images for Paper IV, unfortunately the technology was not always on our side.

I want to thank all the staff at the Department of Radiology, Skåne University Hospital, Lund, for collecting the patient material, especially thanks to Eva, Ann-Charlott and Olivia.

Thanks to the staff at the Department of Radiology in Trelleborg, it is really nice to work with you. Some of you have become my close friends. But I miss our brainstorming sessions, Nyman U, Björkdal P, Åkesson P, Uher R et al.

I would also like to thank those who have been good colleagues in Kristianstad and Hässleholm, where a started my career as a medical physicist. You have assisted with extensive knowledge in radiology and nuclear medicine.

Thanks to my present and past colleagues at the Department of Radiation Physics in Malmö and Lund, Skåne University Hospital and at the Department of Medical Radiation Physics, Lund University. Special thanks to Pântus, Inga, Lars W, Sven M, Mikael, Bengt, Peter W, Magnus O, Sigrid, Christian A, Pernilla, Viveca,

Veronica, Kai, Bea, Christoffer, Hanna, Anja, Sofie, Daniel, Marie S, Hannie, Magnus D, Maria C, Therése, Christian B, Lars H, Martin, Andreas W, Anna H, Carl, Fredrik N, Lena T, Mattias, Simon, David, Jenny, Lena, LEO and Per.

I would also like to thank my former roomie and friend Maria S. I hope we get more time together now then this thesis is completed☺

Jag vill också tacka dem som betyder allra mest för mig, min familj. Mina flickor, Cornelia och Inez, för att ni förgyller mitt liv med busiga upptåg och mys. Anton, för att du alltid ställer upp och hjälper till. Jag uppskattar att du delar min humor och mitt intresse för tvåhjulingar (med motor☺). Bästa Pappa för att du gett mig utmaningar i att tänka ut saker och lösa problem. Finaste Mamma för att du har ett hjärta av guld och för att du är min bästa vän. Ni ställer alltid upp oavsett vad det gäller. Brorsan för att du är du, jag är så stolt över dig. Slutligen, min älskade man Jesper, tack för ditt tålamod och stöd.

# References

- AAPM: American Association of Physicists in Medicine (2011). Size-specific dose estimates (SSDE) in pediatric and adult body CT examinations. AAPM Report No 204.
- AAPM: American Association of Physicists in Medicine (2012). Adult routine head CT protocols. Version 1.1 ed.
- AAPM: American Association of Physicists in Medicine (2014). Use of water equivalent diameter for calculating patient size and size-specific dose estimates (SSDE) in CT. AAPM Report No 220.
- Almén A, Richter S and Leitz W (2008). Number of radiological examinations in Sweden. Swedish Radiation Protection Authority report 2008: 03 (In Swedish).
- Angel E (2012). AIDR 3D Iterative Reconstruction: Integrated, Automated and Adaptive Dose Reduction. Toshiba Medical Systems.
- Aurumskjöld M-L, Ydström K, Tingberg A and Söderberg M (2017). Improvements to image quality using hybrid and model-based iterative reconstructions: a phantom study. *Acta Radiol* 58(1): 53-61.
- SSM, Swedish Radiation Protection Authority (2009). The Swedish Radiation Protection Authority's regulations and general advice on diagnostic standard doses and reference levels within medical X-ray diagnostics. SSM FS 2008:20.
- Bahn Y E, Kim S H, Kim M J, Kim C S, Kim Y H and Cho S H (2015). Detection of urothelial carcinoma: Comparison of reduced-dose iterative reconstruction with standard-dose filtered back projection. *Radiology* 279(2): 471-480.
- Barrett J F and Keat N (2004). Artifacts in CT: recognition and avoidance. *Radiographics* 24(6): 1679-1691.
- Båth M and Hansson J (2016). VGC analyzer: A software for statistical analysis of fully crossed multiple-case visual grading characteristics studies. *Radiat Prot Dosimetry* 169(1-4): 46-53.
- Båth M and Månsson L G (2007). Visual grading characteristics (VGC) analysis: a non-parametric rank-invariant statistical method for image quality evaluation. *Br J Radiol* 80(951): 169-176.
- Dodge C T, Tamm E P, Cody D D, Liu X, Jensen C T, Wei W, Kundra V and Rong X J (2016). Performance evaluation of iterative reconstruction algorithms for achieving CT radiation dose reduction - a phantom study. *Journal of applied clinical medical physics* 17(2): 511-531.
- Droegge R T and Morin R L (1982). A practical method to measure the MTF of CT scanners. *Med Phys* 9(5): 758-760.

- European Commission (2000). European guidelines on quality criteria for computed tomography. Publications of the European Communities. Report EUR 16262 EN.
- Fleischmann D and Boas F E (2011). Computed tomography- old ideas and new technology. *Eur Radiol* 21(3): 510-517.
- Funama Y, Taguchi K, Utsunomiya D, Oda S, Yanaga Y, Yamashita Y and Awai K (2011). Combination of a low-tube-voltage technique with hybrid iterative reconstruction (iDose) algorithm at coronary computed tomographic angiography. *J Comput Assist Tomogr* 35(4): 480-485.
- Gandhi N S, Baker M E, Goenka A H, Bullen J A, Obuchowski N A, Remer E M, Coppa C P, Einstein D, Feldman M K and Kanmaniraja D (2016). Diagnostic accuracy of CT enterography for active inflammatory terminal ileal Crohn disease: comparison of full-dose and half-dose images reconstructed with FBP and half-dose images with SAFIRE. *Radiology* 280(2): 436-445.
- Gervaise A, Osemont B, Lecocq S, Noel A, Micard E, Felblinger J and Blum A (2012). CT image quality improvement using Adaptive Iterative Dose Reduction with wide-volume acquisition on 320-detector CT. *Eur Radiol* 22(2): 295-301.
- Grant K and Raupach R (2012). SAFIRE: Sinogram Affirmed Iterative Reconstruction. White paper. Siemens Healthcare.
- Gordon R, Bender R and Herman G T (1970). Algebraic reconstruction techniques (ART) for three-dimensional electron microscopy and X-ray photography. *Journal of theoretical Biology* 29(3): 471IN1477-1476IN2481.
- Habets J, Symersky P, de Mol B A, Mali W P, Leiner T and Budde R P (2012). A novel iterative reconstruction algorithm allows reduced dose multidetector-row CT imaging of mechanical prosthetic heart valves. *Int J Cardiovasc Imaging* 28(6): 1567-1575.
- Hara A K, Paden R G, Silva A C, Kujak J L, Lawder H J and Pavlicek W (2009). Iterative reconstruction technique for reducing body radiation dose at CT: feasibility study. *AJR Am J Roentgenol* 193(3): 764-771.
- Honda O, Yanagawa M, Inoue A, Kikuyama A, Yoshida S, Sumikawa H, Tobino K, Koyama M and Tomiyama N (2011). Image quality of multiplanar reconstruction of pulmonary CT scans using adaptive statistical iterative reconstruction. *Br J Radiol* 84(1000): 335-341.
- Hounsfield G N (1973). Computerized transverse axial scanning (tomography). 1. Description of system. *Br J Radiol* 46(552): 1016-1022.
- Hsieh J (2003). Investigation of an image artefact induced by projection noise inhomogeneity in multi-slice helical computed tomography. *Phys Med Biol* 48(3): 341-356.
- Hsieh J (2008). Adaptive Statistical Iterative Reconstruction. White paper, GE Healthcare.
- Håkansson M, Svensson S, Zachrisson S, Svalkvist A, Båth M and Månsson L G (2010). VIEWDEX: an efficient and easy-to-use software for observer performance studies. *Radiat Prot Dosimetry* 139(1-3): 42-51.
- ICRP: International Commission on Radiological Protection (1991). Recommendations of the International Commission on Radiological Protection. ICRP Publication 60. *Ann. ICRP* 21 (1-3).

- ICRP: International Commission on Radiological Protection (2000). Managing patient dose in computed tomography. ICRP Publication 87. Ann. ICRP 30 (4).
- ICRP: International Commission on Radiological Protection (2007a). Managing patient dose in multi-detector computed tomography (MDCT). Publication 102. Ann. ICRP 37(1).
- ICRP: International Commission on Radiological Protection (2007b). The 2007 recommendations of the International Commission on Radiological Protection. Publication 103. Ann. ICRP 37(2-4).
- IEC: International Electrotechnical Commission (2009). Medical electrical equipment. Part 2-44: Particular requirements for basic safety and essential performance of X-ray equipment for computed tomography. IEC 60691-2-44. Third edn.
- Irwan R, Nakanishi S and Blum A (2011). AIDR 3D - Reduces Dose and Simultaneously Improves Image Quality. Toshiba Medical Systems.
- Jensen K, Martinsen A C T, Tingberg A, Aaløkken T M and Fosse E (2014). Comparing five different iterative reconstruction algorithms for computed tomography in an ROC study. *European Radiology* 24(12): 2989-3002.
- Kak A and Slaney M (1988). Principles of Computerized Tomographic Imaging. Piscataway, NJ: IEEE Press.
- Kalender W A, Buchenau S, Deak P, Kellermeier M, Langner O, van Straten M, Vollmar S and Wilharm S (2008). Technical approaches to the optimisation of CT. *Phys Med* 24(2): 71-79.
- Kalra M K, Woisetschlager M, Dahlstrom N, Singh S, Digumarthy S, Do S, Pien H, Quick P, Schmidt B, Sedlmair M, Shepard J A and Persson A (2013). Sinogram-affirmed iterative reconstruction of low-dose chest CT: effect on image quality and radiation dose. *AJR Am J Roentgenol* 201(2): 235-244.
- Kalra M K, Woisetschlager M, Dahlstrom N, Singh S, Lindblom M, Choy G, Quick P, Schmidt B, Sedlmair M, Blake M A and Persson A (2012). Radiation dose reduction with Sinogram Affirmed Iterative Reconstruction technique for abdominal computed tomography. *J Comput Assist Tomogr* 36(3): 339-346.
- Kilic K, Erbas G, Guryildirim M, Arac M, Ilgit E and Coskun B (2011). Lowering the dose in head CT using adaptive statistical iterative reconstruction. *AJNR Am J Neuroradiol* 32(9): 1578-1582.
- Kim H G, Lee H J, Lee S K, Kim H J and Kim M J (2017). Head CT: Image quality improvement with ASIR-V using a reduced radiation dose protocol for children. *Eur Radiol* 27(9): 3609-3617.
- Kopp A, Klingenberg-Regn K, Heuschmid M, Kuttner A, Ohnesorge B, Flohr T, Schaller S and Claussen C (2000). Multislice computed tomography: basic principles and clinical applications. *Electromedica-Erlangen* - 68(2): 94-105.
- Korn A, Fenchel M, Bender B, Danz S, Hauser T K, Ketelsen D, Flohr T, Claussen C. D, Heuschmid M, Ernemann U and Brodoefel H (2012). Iterative reconstruction in head CT: image quality of routine and low-dose protocols in comparison with standard filtered back-projection. *AJNR Am J Neuroradiol* 33(2): 218-224.
- Kwon H, Cho J, Oh J, Kim D, Cho J, Kim S, Lee S and Lee J (2015). The adaptive statistical iterative reconstruction-V technique for radiation dose reduction in abdominal CT:

- comparison with the adaptive statistical iterative reconstruction technique. *Br J Radiol* 88(1054): 20150463.
- Li K, Tang J and Chen G H (2014). Statistical model based iterative reconstruction (MBIR) in clinical CT systems: Experimental assessment of noise performance. *Med Physics* 41(4): 041906.
- Little M P, Wakeford R, Tawn E J, Bouffler S D and Berrington de Gonzalez A (2009). Risks associated with low doses and low dose rates of ionizing radiation: why linearity may be (almost) the best we can do. *Radiol* 251(1): 6-12.
- Löve A, Siemund R, Höglund P, Van Westen D, Stenberg L, Petersen C and Björkman-Burtscher I. M (2014). Hybrid iterative reconstruction algorithm in brain CT: a radiation dose reduction and image quality assessment study. *Acta Radiol* 55(2): 208-217.
- Maeda E, Tomizawa N, Kanno S, Yasaka K, Kubo T, Ino K, Torigoe R and Ohtomo K (2017). The feasibility of Forward-projected model-based Iterative Reconstruction Solution (FIRST) for coronary 320-row computed tomography angiography: A pilot study. *J Cardiovasc Comput Tomogr* 11(1): 40-45.
- Martini K, Barth B. K, Higashigaito K, Baumüller S, Alkadhi H and Frauenfelder T (2017). Dose-Optimized Computed Tomography for Screening and Follow-Up of Solid Pulmonary Nodules in Obesity: A Phantom Study. *Curr Probl Diagn Radiol* 46(3): 204-209.
- Mathews J D, Forsythe A V, Brady Z, Butler M W, Goergen S K, Byrnes G B, Giles G G, Wallace A B, Anderson P R, Guiver T A, McGale P, Cain T M, Dowty J G, Bickerstaffe A C and Darby S C (2013). Cancer risk in 680,000 people exposed to computed tomography scans in childhood or adolescence: data linkage study of 11 million Australians. *BMJ* 346: f2360.
- McNitt-Gray M (2006). MO-A-ValB-01: Tradeoffs in Image Quality and Radiation Dose for CT. *Medical Physics* 33(6): 2154-2155.
- Mehta D, Thompson R, Morton A, Dhanantwari A and Shefer E (2013). Iterative model reconstruction: simultaneously lowered computed tomography radiation dose and improve image quality. *Med Phys Inter J* 2013-02: 147-155.
- Miglioretti D L, Johnson E, Williams A, Greenlee R T, Weinmann S, Solberg L I, Feigelson H S, Roblin D, Flynn M. J, Vanneman N and Smith-Bindman R (2013). The use of computed tomography in pediatrics and the associated radiation exposure and estimated cancer risk. *JAMA Pediatr* 167(8): 700-707.
- Miglioretti D L and Smith-Bindman R (2011). Overuse of computed tomography and associated risks. *Am Fam Physician* 83(11): 1252-1254.
- Moscariello A, Takx R A, Schoepf U J, Renker M, Zwerner P L, O'Brien T X, Allmendinger T, Vogt S, Schmidt B, Savino G, Fink C, Bonomo L and Henzler T (2011). Coronary CT angiography: image quality, diagnostic accuracy, and potential for radiation dose reduction using a novel iterative image reconstruction technique-comparison with traditional filtered back projection. *Eur Radiol* 21(10): 2130-2138.
- Nelson R C, Feuerlein S and Boll D T (2011). New iterative reconstruction techniques for cardiovascular computed tomography: how do they work, and what are the advantages and disadvantages? *J Cardiovasc Comput Tomogr* 5(5): 286-292.

- Noel P B, Fingerle A A, Renger B, Munzel D, Rummeny E J and Dobritz M (2011). Initial performance characterization of a clinical noise-suppressing reconstruction algorithm for MDCT. *AJR Am J Roentgenol* 197(6): 1404-1409.
- Oda S, Weissman G, Vembar M and Weigold W G (2014). Iterative model reconstruction: improved image quality of low-tube-voltage prospective ECG-gated coronary CT angiography images at 256-slice CT. *Eur J Radiol* 83(8): 1408-1415.
- Olsson M-L and Norrgren K (2012). An investigation of the iterative reconstruction method iDose<sup>4</sup> on a Philips CT Brilliance 64 using a Catphan 600 phantom. SPIE Medical Imaging, International Society for Optics and Photonics.
- Olsson M-L, Norrgren K, Söderberg, M (2014). Improvement of CT image quality with iterative reconstruction iDose<sup>4</sup>. Poster session presented at European Congress of Radiology, Vienna. Poster retrieved at <http://dx.doi.org/10.1594/ecr2014/C-0387>
- Pan X, Sidky E Y and Vannier M (2009). Why do commercial CT scanners still employ traditional, filtered back-projection for image reconstruction? *Inverse Probl* 25(12): 1230009.
- Park H J, Lee J M, Park S B, Lee J B, Jeong Y K and Yoon J H (2016). Comparison of Knowledge-based Iterative Model Reconstruction and Hybrid Reconstruction Techniques for Liver CT Evaluation of Hypervascular Hepatocellular Carcinoma. *J Comput Assist Tomogr* 40(6): 863-871.
- Pearce M S, Salotti J A, Little M P, McHugh K, Lee C, Kim K P, Howe N L, Ronckers C M, Rajaraman P, Sir Craft A W, Parker L and Berrington de Gonzalez A (2012). Radiation exposure from CT scans in childhood and subsequent risk of leukaemia and brain tumours: a retrospective cohort study. *Lancet* 380(9840): 499-505.
- Pickhardt P J, Lubner M G, Kim D H, Tang J, Ruma J A, del Rio A M and Chen G H (2012). Abdominal CT with model-based iterative reconstruction (MBIR): initial results of a prospective trial comparing ultralow-dose with standard-dose imaging. *AJR Am J Roentgenol* 199(6): 1266-1274.
- Pierce D A, Shimizu Y, Preston D L, Vaeth M and Mabuchi K (2012). Studies of the mortality of atomic bomb survivors. report 12, part I. Cancer: 1950-1990. 1996. *Radiat Res* 178(2): Av61-87.
- Pontana F, Duhamel A, Pagniez J, Flohr T, Faivre J B, Hachulla A L, Remy J and Remy-Jardin M (2011). Chest computed tomography using iterative reconstruction vs filtered back projection (Part 2): image quality of low-dose CT examinations in 80 patients. *Eur Radiol* 21(3): 636-643.
- Pontana F, Pagniez J, Flohr T, Faivre J B, Duhamel A, Remy J and Remy-Jardin M (2011). Chest computed tomography using iterative reconstruction vs filtered back projection (Part 1): Evaluation of image noise reduction in 32 patients. *Eur Radiol* 21(3): 627-635.
- Prakash P, Kalra M K, Kambadakone A K, Pien H, Hsieh J, Blake M A and Sahani D V (2010). Reducing abdominal CT radiation dose with adaptive statistical iterative reconstruction technique. *Invest Radiol* 45(4): 202-210.
- Ren Q, Dewan S K, Li M, Li J, Mao D, Wang Z and Hua Y (2012). Comparison of adaptive statistical iterative and filtered back projection reconstruction techniques in brain CT. *Eur J Radiol* 81(10): 2597-2601.

- Sagara Y, Hara A K, Pavlicek W, Silva A C, Paden R G and Wu Q (2010). Abdominal CT: comparison of low-dose CT with adaptive statistical iterative reconstruction and routine-dose CT with filtered back projection in 53 patients. *AJR Am J Roentgenol* 195(3): 713-719.
- Samei E and Richard S (2015). Assessment of the dose reduction potential of a model-based iterative reconstruction algorithm using a task-based performance metrology. *Med Phys* 42(1): 314-323.
- Sauter A, Koehler T, Fingerle A A, Brendel B, Richter V, Rasper M, Rummeny E J, Noel P B and Munzel D (2016). Ultra Low Dose CT Pulmonary Angiography with Iterative Reconstruction. *PLoS One* 11(9): e0162716.
- Scheffel H, Stolzmann P, Schlett C L, Engel L C, Major G P, Karolyi M, Do S, Maurovich-Horvat P and Hoffmann U (2012). Coronary artery plaques: cardiac CT with model-based and adaptive-statistical iterative reconstruction technique. *Eur J Radiol* 81(3): e363-369.
- Shah N B and Platt S L (2008). ALARA: is there a cause for alarm? Reducing radiation risks from computed tomography scanning in children. *Curr Opin Pediatr* 20(3): 243-247.
- Shuman W P (2016). Iterative Reconstruction in CT: What Does It Do? How Can I Use It?. Retrieved August, 2017, from <http://www.imagewisely.org/imaging-modalities/computed-tomography/imaging-physicians/articles/adaptive-iterative-reconstruction-in-ct>.
- Shuman W P, Green D E, Busey J M, Kolokythas O, Mitsumori L M, Koprowicz K M, Thibault J, Hsieh J, Alessio A M and Choi E (2013). Model-based iterative reconstruction versus adaptive statistical iterative reconstruction and filtered back projection in liver 64-MDCT: focal lesion detection, lesion conspicuity, and image noise. *American journal of roentgenology* 200(5): 1071-1076.
- Singh S, Kalra M K, Hsieh J, Licato P E, Do S, Pien H H and Blake M A (2010). Abdominal CT: comparison of adaptive statistical iterative and filtered back projection reconstruction techniques. *Radiology* 257(2): 373-383.
- Smith S W (1997). *The scientist and engineer's guide to digital signal processing*. San Diego, California: California Technical Publishing.
- Thibault J, Sauer K D, Bouman C A, Hsieh J (2007). A three-dimensional statistical approach to improved image quality for multislice helical CT. *Med Phys* 34(11): 4526-4544.
- Thibault J (2010). *Vevo CT model-based iterative reconstruction*. White paper, GE Healthcare.
- Utsunomiya D, Weigold W G, Weissman G and Taylor A J (2012). Effect of hybrid iterative reconstruction technique on quantitative and qualitative image analysis at 256-slice prospective gating cardiac CT. *Eur Radiol* 22(6): 1287-1294.
- Vardhanabhuti V, Riordan R D, Mitchell G R, Hyde C and Roobottom C A (2014). Image comparative assessment using iterative reconstructions: clinical comparison of low-dose abdominal/pelvic computed tomography between adaptive statistical, model-based iterative reconstructions and traditional filtered back projection in 65 patients. *Invest Radiol* 49(4): 209-216.

- Verdun F, Racine D, Ott J, Tapiovaara M, Toroi P, Bochud F, Veldkamp W, Schegerer A, Bouwman R and Giron I H (2015). Image quality in CT: From physical measurements to model observers. *Physica Medica* 31(8): 823-843.
- Willemink M J, de Jong P A, Leiner T, de Heer L M, Nievelstein R A, Budde R P and Schilham A M (2013). Iterative reconstruction techniques for computed tomography Part 1: technical principles. *Eur Radiol* 23(6): 1623-1631.
- Vining D and Gladish G W (1992). Receiver operating characteristic curves: a basic understanding. *Radiographics* 12(6): 1147-1154.
- Winklehner A, Karlo C, Puipe G, Schmidt B, Flohr T, Goetti R, Pfammatter T, Frauenfelder T and Alkadhi H (2011). Raw data-based iterative reconstruction in body CTA: evaluation of radiation dose saving potential. *Eur Radiol* 21(12): 2521-2526.
- Yamada Y, Jinzaki M, Hosokawa T, Tanami Y, Sugiura H, Abe T and Kuribayashi S (2012). Dose reduction in chest CT: comparison of the adaptive iterative dose reduction 3D, adaptive iterative dose reduction, and filtered back projection reconstruction techniques. *Eur J Radiol* 81(12): 4185-4195.
- Yanagawa M, Honda O, Kikuyama A, Gyobu T, Sumikawa H, Koyama M and Tomiyama N (2012). Pulmonary nodules: effect of adaptive statistical iterative reconstruction (ASIR) technique on performance of a computer-aided detection (CAD) system-comparison of performance between different-dose CT scans. *Eur J Radiol* 81(10): 2877-2886.
- Yasaka K, Katsura M, Akahane M, Sato J, Matsuda I and Ohtomo K (2013). Model-based iterative reconstruction for reduction of radiation dose in abdominopelvic CT: comparison to adaptive statistical iterative reconstruction. *Springerplus* 2(1): 209.



Computed tomography (CT) is one of the most important diagnostic tools in modern health care. CT is known as a high-dose modality but also produces images with high diagnostic value. The role of accurate investigation and diagnosis in the management of all diseases is unquestionable. Every examination with ionising radiation should be performed with a balance obtaining the necessary diagnostic information while keeping the radiation dose to the patient as low as possible. Dose reduction in CT often results in degradation of the image quality, i.e., higher noise

and lower spatial resolution. Advanced software solutions such as iterative reconstruction methods have been introduced to reduce radiation dose in CT. Filtered back projection has been the most common reconstruction method but is increasingly being replaced by different types of IR methods. This thesis focused on evaluation and optimisation of iterative reconstruction methods in CT regarding image quality and radiation dose to the patient.



**LUND UNIVERSITY**  
Faculty of Medicine

Department of Translation Medicine  
Medical Radiation Physics Malmö  
Skåne University Hospital  
Lund University, Faculty of Medicine  
Doctoral Dissertation Series 2017:116  
ISBN 978-91-7619-499-7  
ISSN 1652-8220

